APPLICATION OF FLUID INCLUSIONS AND MINERAL TEXTURES IN EXPLORATION FOR EPITHERMAL PRECIOUS METALS DEPOSITS

By

Jorge Daniel Moncada de la Rosa

Thesis submitted to the faculty of the Virginia Polytechnic Institute and State University in partial fulfillment of the requirement for the degree of

MASTER OF SCIENCE

In

Geosciences

Committee

Robert J. Bodnar, co-chair
Antonio Nieto, co-chair
J. Donald Rimstidt

December 9, 2008

Blacksburg, VA

Keywords: (Guanajuato, Veta Madre, fluid inclusions, boiling, colloform silica, lattice-bladed calcite, mineral exploration, epithermal precious metals deposits, binary classifier statistical software)

APPLICATION OF FLUID INCLUSIONS AND MINERAL TEXTURES IN EXPLORATION FOR EPITHERMAL PRECIOUS METALS DEPOSITS

Daniel Moncada

ABSTRACT

Fluid inclusion and mineralogical features indicative of boiling have been characterized in 855 samples from epithermal precious metals deposits along the Veta Madre at Guanajuato, Mexico. Features associated with boiling that have been identified at Guanajuato include colloform texture silica, plumose texture silica, moss texture silica, ghost-sphere texture silica, lattice-bladed calcite, lattice-bladed calcite replaced by quartz and pseudo-acicular quartz after calcite and coexisting liquid-rich and vapor-rich fluid inclusions. Most samples were assayed for Au, Ag, Cu, Pb, Zn, As and Sb, and were divided into high-grade and low-grade samples based on the gold and silver concentrations. For silver, the cutoff for high grade was 100 ppm Ag, and for gold the cutoff was 1 ppm Au. The feature that is most closely associated with high grades of both gold and silver is colloform texture silica, and this feature also shows the largest difference in grade between the presence or absence of that feature (178.8 ppm Ag versus 17.2 ppm Ag, and 1.1 ppm Au versus 0.2 ppm Au). For both Ag and Au, there is no significant difference in average grade as a function of whether or not coexisting liquid-rich and vapor-rich fluid inclusions are present.

The textural and fluid inclusion data obtained in this study were analyzed using the binary classifier within SPSS Clementine. The models that correctly predicted high versus low grade samples most consistently (~70-75% of the tests) for both Ag and Au were the neural network, the C5 decision tree and Quest decision tree models. For both

Au and Ag, the presence of colloform silica texture was the variable with the greatest importance, i.e., the variable that has the greatest predictive power.

Boiling features are absent or rare in samples collected along a traverse perpendicular to the Veta Madre. This suggests that if an explorationist observes these features in samples collected during exploration that an environment favorable to precious metal mineralization is nearby. Similarly, good evidence for boiling is observed in the deepest levels of the Veta Madre that have been sampled in the mines and drill cores, suggesting that additional precious metal reserves are likely beneath the deepest levels sampled.

Acknowledgements

I would like to take the time first and foremost to thank my family for supporting me during all these years. I want to thank my mother Martha Agueda de la Rosa Espinoza for all her love and her sacrifice. My advisor, Dr. Robert J. Bodnar for his unselfish help, and I am very grateful for his support and for the experience and knowledge I have gained through last two years.

Staff from Great Panther Resources Ltd., especially Robert Archer, William Vanderwall and Robert Brown, are thanked for providing financial support and access to samples and information.

Jim Reynolds showed me the passionate and important religion of fluid inclusions and Scott Mutchler introduced me to the dark side of mathematics. Charles Farley provided help with Raman analysis.

I thank CONACYT and the Virginia Tech Graduate School for providing funding during this study.

I thank the office staff, especially Mary McMurray who helped with travel issues and Connie Lowe for advice and other work that she is doing all the time to help me.

My committee members, Dr. J. Donald Rimstidt and Dr. Antonio Nieto are thanked for their support and for discussions that improved the quality of my research.

I am very grateful to my wife, Elva being always there for me, especially in the difficult moments. Thanks for all your patience, support, and love that helped me to accomplish this thesis.

My fellow graduate students and members of the Fluids Research Laboratory, Rosario Esposito, Max Rolandi, Andras Fall, Martin Hernandez-Marin, Rocky Severs, Steve Becker, Claudia Cannatelli, Jason Lunze, Matthew Steele-MacInnis, John Wyatt, Luca Fedele, all helped during difficult times.

In memory of Guillermo García Figueroa.

Table of Contents

List of Tables

List of Figures

Introduction

Over the past several decades there have been numerous studies of fluids and fluid inclusions in both active terrestrial geothermal systems and their fossil equivalents, the epithermal precious metals deposits (Roedder, 1984; Hedenquist et al., 2000; Albinson et al., 2001; Simmons et al., 2005). There is now a large database of fluid properties in these systems that documents the close association between boiling and mineralization in the epithermal environment. Once boiling begins at depth, the fluid will usually continue to boil to the surface (Figure 1), assuming that the system is composed of interconnected open fractures and is at hydrostatic pressure (Fournier, 1985; Henley and Brown, 1985; Vikre, 1985; Cline et al., 1992). Above the boiling horizon low to moderate salinity liquid and a low density vapor coexist. Fluid inclusion assemblages trapped from the boiling horizon to the surface are characterized by coexisting liquid-rich and vapor-rich inclusions that generally homogenize at =300°C near the base of the boiling zone (Fig. 1) (Bodnar et al., 1985; Simmons and Christenson, 1994), to <220°C near the top of the system (Albinson et al., 2001), and provide a valuable tool in exploration for epithermal deposits (Roedder and Bodnar, 1997). At depths beneath the boiling horizon, fluid inclusion assemblages are characterized by inclusions with consistent liquid-to vapor ratios that homogenize to the liquid phase, often at temperatures greater than 300°C (Bodnar et al., 1985). Note that hydrothermal systems associated with the formation of epithermal deposits are dynamic systems, and the boiling horizon likely shifts upward and downward over time as the fluid temperature, flow rate, fracture apertures, etc., vary through time.

The salinity of the hydrothermal fluid in epithermal deposits varies over a broad range and can be related to the metal budget of the system. The salinity above the boiling horizon is generally <23 wt.% NaCl equivalent, and often <5 wt.%, whereas the salinity at bottom of the system is usually between 10-20 wt% NaCl equivalent (Albinson et al., 2001). The salinity is typically lower in gold-rich (or gold-only) systems and increases with both increasing Ag/Au ratio and base metal / precious metal ratio (Albinson et al., 2001).

The boiling horizon not only represents a change in the fluid inclusion types that are observed, but also represents a change in ore metal distribution with depth. Beneath the boiling horizon many systems are characterized by higher base metal and lower (or absent) precious metal grades, whereas above the boiling horizon precious metals are more common. The highest gold grades are often found immediately above the boiling horizon (Buchanan, 1981; Cline et al., 1992; Hedenquist et al., 2000). Albinson et al. (2001) note that ore zones in boiling epithermal systems often show an economic bottom that is characterized by a dramatic change from high-grade ore to barren rock over a few meters depth, whereas in the less common non-boiling epithermal deposits the economic bottom of the deposit occurs due to the gradual decrease in ore grade with depth.

The spatial relationship between boiling, fluid inclusion characteristics and precious metal mineralization provides a potentially valuable tool in exploration for epithermal precious metals deposits. Thus, the presence of fluid inclusions indicative of boiling in surface outcrops suggests that the base of the boiling zone, and the location in the hydrothermal system where highest precious metal grades are most likely to occur if the system is mineralized, will be at depth. Conversely, if an epithermal quartz vein at the

surface shows no evidence for the presence of boiling fluids, either in the fluid inclusion record or mineral textures, it is unlikely that boiling occurred at greater depths in the vein system. In this case, the quartz vein would not represent a high priority target for further exploration.

One of the locations where the temporal and spatial association of boiling and precious metal deposition in epithermal deposits was first recognized was in the Finlandia vein, Peru. There, Kamilli and Ohmoto (1977) identified seven distinct stages of alteration and mineralization. Boiling, as evidenced by coexisting liquid-rich and vapor-rich inclusions with variable phase ratios, was only recognized in the stage II bonanza Ag-Au stage. These workers concluded that the precipitation of Ag-Au ore was caused by boiling of hydrothermal fluids with salinities ranging from 0.2 to 13 wt. % NaCl equivalent at temperatures between 250 ºC and 310 ºC (Kamilli and Ohmoto, 1977).

Similarly, in the National District in the Buckskin Mountains, Nevada, Vikre (1985) reported that boiling did not occur in the early pre- Au-Ag stage (stage 1). However, coexisting liquid-rich and vapor-rich inclusions with homogenization temperatures ranging from 250 to 295ºC were observed in stages 2-4 that are associated with Au and Ag mineralization. Importantly, the paleosurface at the time of mineralization is still recognizable in this young system, and boiling is observed from a depth of 2,000 feet all the way to the surface.

It is important to note that not all epithermal precious metals deposits show an association between boiling and mineralization, as Albinson et al. (2001) have documented for some Mexican silver deposits. Similarly, Casadevall and Ohmoto (1977) found no evidence of boiling associated with precious metals deposition (stage 4) in the

Sunnyside, Colorado, epithermal deposit. They did, however, report boiling during the latest stage 6 that contains no precious metal mineralization.

During the past half century several workers have studied fluid inclusions in the Guanajuato Mining District (GMD) (Table 1). One of the earliest studies, by Wilson et al. (1950), focused on mines in the central part of GMD (Fig. 2). Thirty samples containing quartz crystals from the Rayas mine and the Cata mine showed homogenization temperatures ranging from 215 to 299 ºC, with an average of 254 ºC and a mean of 257 ºC. These workers did not comment on whether the samples contained both liquid-rich and vapor-rich inclusions in the same assemblages.

Gross (1975) reported fluid inclusion homogenization temperatures from several samples collected along the Veta Madre and adjacent Sierra vein system (Fig. 2). Temperatures ranged from about 260 to 330°C and showed a systematic increase with depth. For example, the temperature at an elevation of 1700 m was 320°C and dropped to 260°C at 2400 m along the Veta Madre. As with the earlier work by Wilson et al. (1950), Gross (1975) did not indicate whether the samples contained both liquid-rich and vapor-rich inclusions in the same assemblages.

The most detailed fluid inclusion study in the GMD and the first that relates boiling and precipitation of precious metals was conducted by Buchanan (1979), whose research focused on the Las Torres mine and the deepest levels of the Rayas mine (1705 meter level) (Fig. 2). In both mines, coexisting liquid-rich and vapor-rich inclusions indicated that boiling occurred during precious metal mineralization. In the Las Torres mine, a correlation was observed between silver sulfide deposition, high abundance of fluid inclusions with homogenization temperatures ranging from 231 to over 360 ºC, and

deposition of adularia and sericite. In addition, a sample from the Rayas mine collected at an elevation of 1705 m showed evidence of boiling and homogenization temperatures from 290 to 385 ºC. Twelve other samples from the Rayas mine contained vapor-rich inclusions but these were interpreted to have formed by necking down (Buchanan, 1979). Two boiling horizons were observed in the Las Torres Mine. The shallow horizon was interpreted to represent "normal" hydrostatic boiling, whereas the deeper horizon was thought to represent flashing of the hydrothermal fluids when the impermeable seal fractured. The boundary between the boiling zone (above) and the non-boiling zone (below) was located at an elevation of about 1800 m (Buchanan, 1979).

In contrast to the observations of Buchanan (1979; 1980), Mango (1988) and Mango et al. (1991) found no evidence of boiling in fluid inclusions in quartz, calcite, and sphalerite from the Rayas Mine. Stable isotope analyses indicated that the precious and base-metals were deposited from meteoric water (Mango, 1988). Homogenization temperatures of fluid inclusions range from 230 to 305 ºC and have a salinity of 1.2 wt. % NaCl equivalent. Results from gas analysis showed 0.3 to 2.1 mole % CO_2, 0.06 to 0.8 mole % H_2S, and less than 1 mole % CH_4, H_2 and CO in the inclusions (Mango et al., 1991). Mango et al. (1991) reported that boiling did not occur at any of the levels studied at Rayas, and suggest that if boiling of the hydrothermal fluids did occur it was at higher stratigraphic levels which have since been eroded. These workers also report that up to 850 m of erosion may have occurred above the Rayas orebody, and Buchanan (1981) indicated that boiling only occurred to a depth of 650 m below the surface at the time of mineralization. It should be noted that Rayas contains more base metal sulfides than some other mines in the GMD (i.e., Las Torres), and less gold than others (i.e., El Cubo).

Recently, several fluid inclusion studies have been conducted along the Sierra vein system that parallels the Veta Madre in the GMD. In the Cubo Mine the San Nicolas vein is oriented perpendicular (east-west) to the Veta Madre vein (Fig. 2). Most fluid inclusions from this vein homogenize at about 250°C (Girnius, 1993), and evidence for boiling was only found in samples from the western-most portion of the vein. Girnius (1993) interpreted these data to indicate that deposition was the result of both fluid mixing and boiling. More recently, Abeyta (2003) studied the San Nicolas vein and reported homogenization temperatures of 172 – 282°C and salinities of 0 – 3 wt% NaCl equivalent. Abeyta (2003) noted the presence of coexisting liquid-rich and vapor-rich inclusions as well as bladed calcite in the veins and interpreted this to indicate boiling.

Perhaps one of the best examples of the close association between boiling and precious metal deposition in the epithermal environment is provided by the modern geothermal systems in New Zealand. There, a new back-pressure plate was installed in the high-pressure part of a well in the Ohaaki-Broadlands geothermal field. The back-pressure plate is located at the point where high temperature one-phase liquid geothermal fluids "flash" (boil) to produce steam at the wellhead. After 44 days the plate was removed and the scales were analyzed. The scale was mostly chalcopyrite, containing about 4-6 wt% Au and 2.5-30 wt% Ag. Brown (1986) concluded that the sudden flashing that converts hot water to steam resulted in metal precipitation.

Fluid inclusion studies and studies of active geothermal systems summarized above document the generally recognized spatial and temporal relationship between boiling and precious metal mineralization. This relationship is consistent with theoretical and experimental studies of gold solubility. Gold solubility at 250°C as a function of fluid

pH and oxidation state is shown on Figure 3. Also shown on Figure 3 are the stability fields for Fe-bearing phases hematite, pyrite, magnetite and pyrrhotite for a total sulfur activity of 0.01. Illite and adularia are common alteration and gangue minerals in epithermal systems, and the illite-adularia equilibrium boundary is shown for both equilibrium with amorphous silica and quartz at 250°C, assuming K^+ concentration of 5 x 10^{-3} *m* and Mg^{2+} concentration of 4 x 10^{-5} *m*. Illite-adularia equilibria were calculated using data from Helgeson (1969) combined with the data from Gunnarsson and Arnórsson (2000) for quartz and amorphous silica equilibria. Note that the pH of a fluid in equilibrium with illite and adularia and precipitating quartz will decrease by greater than one pH unit if the fluid suddenly begins to precipitate amorphous silica in response to boiling. This results in a decrease in the gold solubility of about 1-2 orders of magnitude and can cause gold to precipitate. Also shown o Figure 3 are the $H_2S - HS^-$ and $HSO^-_4 - SO^{2-}_4$ equilibrium boundaries. In most epithermal deposits, pyrite or an iron oxide phase and adularia are common gangue minerals (Sillitoe and Hedenquist, 2003). Gold solubilities shown on Figure 3 are consistent with Au concentrations in deep geothermal waters in the Taupo Volcanic Zone and at Lihir Island, Papua New Guinea (Simmons, and Brown, 2008).

According to Figure 3, the maximum gold solubility occurs near the intersection of the hematite and pyrite fields and decreases in all directions away from this maximum. Assuming a fluid is saturated in gold at this maximum, any process that causes the fluid composition to move away from that point results in a decrease in solubility and deposition of gold. Thus, gold can be deposited if the fluid pH increases or decreases, or if the oxygen fugacity increases or decreases (Fig. 3). Assuming that gold is transported

as a bisulfide complex, boiling of a solution results in consumption of hydrogen ion (pH increases) and loss of the complexing agent for gold according to equation (1)

$$Au(HS)_2^- + 0.5\ H_2 + H^+ = Au\ (s) + H_2S\ (v) \qquad (1)$$

Boiling also results in loss of CO_2 from the solution which in turn leads to a pH increase according to equation (2)

$$HCO_3^- + H^+ = H_2O + CO_2\ (v) \qquad (2)$$

Pyrite precipitation also promotes gold deposition by removing the complexing agent (sulfur) responsible for transporting gold (Henley and Brown, 1985) according to equation (3)

$$Fe^{2+} + 2Au(HS)_2^- = 2Au\ (s) + FeS_2\ (s) + 2H^+ + 2HS^- \qquad (3)$$

Most epithermal ore-forming fluids are probably not saturated in Au initially, but rather achieve saturation and deposit gold as a result of changes in the chemical and physical environment at the site of deposition. However, as noted above, boiling, pyrite deposition and a change from quartz to amorphous silica deposition all require changes in the pH and/or sulfur activity of the fluid, which can lead to gold deposition.

The discussion above applies only to gold solubility and deposition. The mechanisms by which silver is dissolved and transported in epithermal systems, on the

other hand, are not as well understood. If silver is transported as a sulfide complex, boiling should also cause silver to precipitate. However, if silver is transported as a chloride complex boiling is less likely to result in silver precipitation. Recent experimental studies by Pokrovski et al. (2008) at 350 – 500°C (temperatures somewhat higher than those in the epithermal environment) showed that the solubility of silver in chloride solutions decreases with increasing pH, reflecting a change from transport as a chloride complex in acidic solutions to transport as S-complexes in neutral to basic solutions. Thus, the changes in solution properties described above as a result of boiling, specifically an increase in pH, will also promote silver deposition if silver is transported as a sulfur complex.

In this study, the relationship between fluid inclusion and mineral textural evidence for boiling and precious metal grades in the classic epithermal Ag-Au deposits at Guanajuato, Mexico, have been investigated to test for systematic correlations that may be used in exploration for similar deposits. Approximately 850 samples were collected from surface outcrops, underground workings, and recent drill core over a strike length of 4 km and to depths of 750 m beneath the surface in four active mines and one closed mine along the Veta Madre. Each sample was assayed for Au, Ag, Cu, Pb, Zn, As, Sb. The goal of this study was to develop a method to evaluate the economic potential samples based only on data obtained during petrographic examination of thin sections and does not require time-consuming and expensive microthermometry or microanalysis of the inclusions.

Geological Setting

The Guanajuato Mining District (GMD) is located at the southern end of the Sierra Madre Occidental Eocene-Oligocene volcanic province and between the Sierra Madre Oriental and the Trans-Mexican volcanic belt (Clark et al., 1982). The GMD is part of a large northwest trending belt of silver-lead-zinc deposits that parallels the eastern flanks of the Sierra Madre Occidental (Randall et al., 1994). Aranda-Gómez et al. (2003) divide the rocks in this area into a "basal complex" and "cover rocks". The basal complex consists of metamorphosed marine sediments of Mesozoic to early Tertiary age, while the Cenozoic cover rocks are composed of continental sediments and subaerial volcanic rocks. The Cenozoic volcanism has been divided into seven pulses (Aranda-Gómez et al., 2003), ranging in age from about 51 Ma to 8 Ma. Felsic to intermediate volcanism that occurred from 37 to 27 Ma produced the rock units and structures that host the mineral deposits (Godchaux et al., 2003).

The regional geology in the GMD has been studied in detail by Edwards (1955), Echegoyen-Sanchez (1964), Taylor (1971), Gross (1975), Buchanan (1979) and Randall et al. (1994). The lowermost unit present in the area is the Esperanza Formation (Fig. 4) composed of carbonaceous and calcareous mudstones, shales, limestones and andesitic to basaltic flows that have all been metamorphosed to phyllite, slate and marble (Wandke and Martinez, 1928; Randall et al., 1994; Stewart, 2006). The thickness of this unit exceeds 600 m in the GMD and it has been assigned a Cretaceous age based on radiolaria (Dávila and Martínez-Reyes, 1987).

The next youngest unit in the GMD is the La Luz andesite (Randall et al., 1994), but this unit is absent in the vicinity of the city of Guanajuato and along the Veta Madre that is the focus of this study (Buchanan, 1979). In this area, the Guanajuato Formation lies unconformably on the Esperanza Formation (Fig. 4). The Guanajuato Fm. is composed of red, poor- to well-sorted conglomerate, sandstone and shale (Buchanan, 1979). The Guanajuato Fm. ranges from 1500 – 2000 m in thickness and is Eocene to early Oligocene in age based on vertebrate fossils (Edwards 1955).

The Guanajuato Fm. is conformably overlain by the Loseros Fm. (Fig. 4), which is a 10 to 52 m thick, green andesitic volcaniclastic sandstone (Echegoyen-Sanchez, 1964; Buchanan, 1979). While no ages have been determined for the Loseros Fm., it is assumed to be early Oligocene based on its conformable location between the underlying Guanajuato Fm. and overlying Oligocene Bufa Fm.

The Bufa Formation conformably overlies the Loseros Fm. The Bufa Fm. (Fig. 4) represents a 350 m thick distal volcano-sedimentary unit with white, yellow, pink rhyolitc lapilli air-fall ash that has been dated at 37 +/- 3.0 Ma using K-Ar (Gross, 1975). The Bufa Fm. is separated from the overlying Calderones Fm. by a disconformity (Buchanan, 1979). The Calderones Formation consists of chloritized, crystal-rich andesitic tuff, except at the base. Here, andesitic volcanoclastic shale and sandstone lie unconformably on the Bufa Fm. The Calderones Fm. (Fig. 4) is 200-250 m thick (Gross, 1975; Stewart, 2006) and has been assigned a late Oligocene age based on cross-cutting relationships (Gross, 1975).

Overlying the Calderones Fm. is the Cedros Fm. (Fig. 4) which consists of grey to black andesitic flows interbedded with grey to green andesitic tuffs (Buchanan, 1979).

The thickness of this unit is highly variable and ranges from 100 – 240 m in the district (Gross, 1975; Stewart, 2006).

The Chichindaro Fm. (Fig. 4) is the youngest formation in the area and has been dated at 32 +/- 1 Ma by K- Ar (Gross, 1975; Randall et al., 1994). It unconformably overlies the Cedros Formation and is composed of felsic ash and flow breccias (Taylor, 1971). Buchanan (1979) reports that the Chichindaro Fm. is pre-mineralization.

Mineralization in the GMD is associated with three parallel, northwest trending fault systems. The La Luz system is to the north and west of the city of Guanajuato, the Sierra system is to the east and south of the city of Guanajuato, and the intermediate Veta Madre system passes through city of Guanajuato (Fig. 2). All samples studied here were collected from the Veta Madre and along a traverse perpendicular to the vein.

In the study area the Veta Madre dips 35-55° to the SW and varies from hairline to several tens of m in thickness (Buchanan, 1979). The Esperanza Fm., composed of dull-black carbonaceous and calcareous mudstones, shales, limestones and andesitic to basaltic flows that have all been metamorphosed to phyllite, slate and marble, serves as the footwall of the Veta Madre (Guiza, 1949; Edwards 1955; Cornelius, 1964). The Guanajuato Fm., composed of red, poor- to well-sorted conglomerate, sandstone and shale, forms the hanging wall of the Veta Madre (Edwards 1955) (Fig. 5).

The Veta Madre mineralization consists mostly of quartz and silica with lesser calcite, fluorite, barite and adularia. The Veta Madre is composed of multiple generations of mostly silica and carbonate deposition and brecciation to produce veins and stockworks (Stewart, 2006) that are dominated by banded quartz (silica) (Wandke and Martinez, 1928). The banding structures in the veins are closely associated with

mineralization and were an indication to early miners of high grades of ore (Wandke and Martinez, 1928). The stockworks are present in the hanging wall of the main vein and can have stope dimensions of more than 200 m x 100 m (Wandke and Martinez, 1928)

Methodology

Sample Collection and Preparation

Working in collaboration with the staff of Great Panther Resources, a total of 855 samples were collected along a 4 km strike length of the Veta Madre from both surface outcrops (Fig. 5, top) and underground locations, including drill core (Fig 5, bottom). The accessibility of underground workings in the San Vicente, Cata, Valenciana, Rayas and Guanajuatito Mines offered good three dimensional geological controls. The northern part of Valenciana Mine was not accessible because this area was flooded and access was prohibited. Collection of samples from surface outcrops and underground and drill cores focused on samples that contained transparent minerals that could be examined for fluid inclusions, especially quartz and calcite.

Surface samples were collected at each location where vein material was encountered outcropping on the surface (Fig. 5, top). One 400 m traverse perpendicular to the Veta Madre in the vicinity of the San Vicente Mine was also conducted, collecting samples of quartz and/or calcite veins that were encountered along the traverse. In the underground mines, samples were collected at regular intervals along drifts. Sample locations were determined using mine maps and survey marks. Samples were collected from the hanging wall and footwall of the vein where access permitted. Underground areas sampled included the following mines: Rayas Mine (345 and 390 levels), Cata

Mine (390 and 414 levels), south Valenciana Mine (320 level), Guanajuatito Mine and San Vicente Mine (190, 220, 270, 275 and 345 levels) (Fig. 5, bottom). Levels for all mines indicate depth beneath the surface in meters, relative to the elevation at the top of the Rayas shaft, which is at an elevation of 1,999 m above sea level. Drill core samples were obtained from the underground and surface drilling program and historical drilling (Fig. 5, bottom). At each location one "representative" sample was collected, although it should be noted that recognizable heterogeneity occurred over short distances along each level.

The hand samples were cut perpendicular to the vein to produce a section that extended from the vein wall towards the center of the vein. Then a thin section-sized billet approximately 13/16 inches x 1 inch (21 mm x 35 mm) was cut from the larger slab and a "thick" section approximately 75 µm thick was prepared. If the vein thickness was greater then twice the long dimension of the billet, the billet was cut to include one of the vein walls. The logic of this approach is that the material closest to the vein wall is the oldest material in the vein, because these are open-space filling veins and not crack-seal veins. Thus, even if mineralization at that location occurred later than the time represented by the sample, the sample is still likely to contain secondary fluid inclusions containing fluids responsible for precipitating later material. This approach increases the likelihood of sampling all fluid events associated with vein formation while at the same time minimizing the size and/or number of thick sections needed.

Thick section preparation was done by an outside vendor and at Virginia Tech. This study involved only petrographic examination of the samples, thus doubly polished sections were not required. "Quick plates" were prepared (Goldstein and Reynolds, 1994)

by polishing the cut surface with 320 micron grit to eliminate the macroscopic imperfections produced by cutting the sample. Next, the sample was mounted to a glass slide with epoxy adhesive. The final process consisted of cutting and grinding the sections to 75-100 micron thickness (Van den Kerkhof and Hein, 2001) in order to study the fluid inclusions and mineral textures.

In addition to preparing thick sections from the samples, one half of each cut sample was assayed for gold (Au), silver (Ag), copper (Cu), lead (Pb), zinc (Zn), arsenic (As) and antimony (Sb).

Petrography

Goldstein and Reynolds (1994) describe the technique for observing unpolished thick sections ("quick sections") under the microscope that involves covering the surface with immersion oil to improve the optical properties of the sample for viewing fluid inclusions. The immersion oil with an index of refraction equivalent to that of the mineral fills all cracks and imperfections. Because our samples consisted mostly of quartz we used oil with an index of refraction of 1.515.

Samples were examined using a petrographic microscope, starting at low magnification and preceding to higher magnification. The first task for each sample was to identify the minerals and to classify the textures of quartz and calcite if present (every sample contained quartz and about one-quarter also contained calcite). Next, the sample was examined systematically to identify fluid inclusion assemblages (FIAs) and the types of fluid inclusions in each FIA were noted. An FIA represents a group of fluid inclusions that were all trapped at the same time (Goldstein and Reynolds, 1994; Bodnar, 2003a)

and thus represent the physical and chemical conditions in the system at the time trapping. FIAs may be composed of primary inclusions trapped during precipitation of the host phase, or may contain secondary inclusions that are trapped along fractures in the host phase at some time after the mineral has formed. FIAs in samples from the Veta Madre were further classified as containing either only liquid-rich inclusions with consistent liquid-to-vapor ratios, or containing coexisting liquid-rich and vapor-rich inclusions with a broad range in liquid-to-vapor ratios (Fig. 6). Finally, the homogenization temperature of the fluid inclusions was estimated based on the liquid-to-vapor ratio in the fluid inclusions at room temperature (Bodnar, 1983) (Fig. 6).

Fluid inclusions in the Veta Madre, and in all epithermal deposits, must be interpreted with caution because much of the host material was originally deposited as an amorphous silica phase or as fine-grained chalcedony and has since (re-) crystallized to produce coarse-grained quartz. Primary-appearing inclusions in such samples are unlikely to record the original formation conditions (Bodnar et al., 1985; Sander and Black, 1988). In this study, only secondary inclusions that clearly crosscut quartz crystal boundaries, and therefore were trapped after the quartz (re-) crystallized, were studied in quartz that showed textures indicative of original precipitation as an amorphous or fine-grained phase, as described below. Similar arguments apply to fluid inclusions in replacement minerals, such as quartz replacing lattice-bladed calcite.

Silica and calcite textures:

Previous workers have shown that silica and carbonate phases in the epithermal environment can have highly variable and sometimes diagnostic textures (Figs. 7 and 8)

that identify the physical conditions associated with mineralization (Adams, 1920; Bodnar et al., 1985; Sander and Black, 1988; Dong et al., 1995; Simmons and Christenson, 1994; Henley and Hughes, 2000). These various textures can be divided into those that are produced during the original deposition of the phase, those that represent recrystallization textures, and those that represent replacement of originally precipitated material. Further, some of these textures are readily apparent in hand samples, others require microscopic observation, with some are only revealed under crossed-polars. Finally, some of these phases contain fluid inclusions that may be used to infer the paleo-environment in the hydrothermal system, whereas others rarely contain useful fluid inclusions. In this study, we have characterized the mineralogy and mineral textures observable under the microscope, and these are summarized below.

The most common mineral texture observed in 752 out of 855 samples (Fig. 9) from the Veta Madre is mosaic or jigsaw-textured quartz (Figs. 7A). This recrystallization texture is characterized by aggregates of microcrystalline to crystalline quartz crystals with interpenetrating grain boundaries (Dong et al., 1995) that is only recognizable when observed under crossed polars (Fig. 8A, B). The texture is interpreted to result from the recrystallization of massive chalcedony or amorphous silica (Dong et al., 1995). In some cases the original colloform texture is readily apparent in plain polarized light. As noted by Sander and Black (1988), primary fluid inclusions in this type of quartz do not record the original depositional conditions. However, in this study we observed many trails of secondary fluid inclusions in jigsaw quartz that record fluid conditions in the Veta Madre after recrystallization of the original chalcedony or

amorphous silica. As such, these fluid inclusions are useful monitors of the fluid conditions during the later stages of the hydrothermal history of the system.

The next most abundant texture (549 samples; Fig. 9) is plumose quartz texture (Sander and Black, 1988) that shows variable extinction positions when observed under crossed polars (Figs. 7C,D). This silica texture has also been referred to as “feathery” (Fig. 7B) or “flamboyant” (Fig. 7C) by Adams (1920) and Dong et al. (1995). This recrystallization texture is thought to develop from aggregates of fibrous chalcedony with rounded external surfaces which originate as silica gel (Dong et al., 1995). The silica gel is originally precipitated when silica supersaturation occurs in response to rapid cooling and concomitant pressure decrease followed by precipitation of amorphous silica (Henley and Hughes, 2000). As with the jigsaw texture described earlier, primary fluid inclusions in this type of quartz do not record the original depositional conditions, but secondary inclusions provide information concerning later conditions.

Rhombic calcite crystals (Fig. 7E) are observed in 190 out 855 samples from the Veta Madre. While bladed calcite is thought to be characteristic of deposition from a boiling solution (see below), an association between rhombic calcite and boiling is less clear. Fluid inclusions were observed in this mineral but were not recorded because of the ease with which fluid inclusions in calcite, and other soft minerals with perfect cleavage, reequilibrate, both in nature and during sample preparation and analysis in the laboratory (Ulrich and Bodnar, 1988; Bodnar, 2003b).

Colloform texture silica is observed in 193 out of 855 samples from the Veta Madre. Rogers (1918) introduced the term “colloform” to describe silica with a rounded or botryoidal form that occurs in continuous bands (Fig. 7G, 8J). When observed under

crossed-polars, the colloform texture sometimes shows an evolution from fine-grained silica to coarse-grained quartz with a plumose texture (Fig. 7H) along a traverse from the vein wall to the center of the vein. Similarly, colloform texture silica sometimes shows a jigsaw texture characterized by banding of fine-grained silica near the wallrock contact, with the size of grains increasing towards the vein center, and is most easily recognized when the sample is viewed under crossed polars (Fig. 7I). Henley and Hughes (2000) suggest that this texture is generated during rapid opening of a fracture that produces a pressure drop and rapid cooling. Colloform texture silica is a primary depositional texture that has been interpreted to indicate rapid, low temperature deposition of chalcedonic silica in open space in shallow epithermal systems to produce the rhythmic banding (Roedder, 1984; Bodnar et al., 1985; Fournier, 1985). This type of silica contains no useful fluid inclusions (Bodnar et al., 1985).

Lattice bladed calcite is observed in 120 out of 855 samples from the Veta Madre. This classification includes bladed calcite that is still calcite today (Fig. 7F, 8E,F), as well as bladed calcite that has been replaced by quartz (Fig. 7F, 8G,H), and calcite with an acicular texture that has been replaced by quartz (Fig. 7P, 8I). Simmons and Christenson (1994) described the close association between bladed (platy) calcite and boiling in geothermal systems and attributed this morphology to the rapid growth of calcite as carbon dioxide is lost to the vapor phase during boiling. The presence of coexisting liquid-rich and vapor-rich inclusions in the calcite often confirms that the fluids were boiling during bladed calcite formation (Simmons and Christenson, 1994; Simmons et al., 2005). Often quartz completely replaces the bladed calcite and this is thought to occur in the presence of non-boiling fluids, after precipitation of small quartz and adularia crystals

on the original calcite blades during the latter stages of boiling (Etoh et al., 2002). This type of replacement texture contains no useful primary fluid inclusions, but secondary inclusions provide information concerning later conditions. The pseudo-acicular replacement texture (Fig. 7P, 8I) is produced when parallel bladed calcite or rhombic calcite is replaced by silica. An aggregate of fine-grained silica phases with anhedral to rectangular shape replace the calcite to produce an acicular morphology (Adams, 1920; Dong et al., 1995). This type of replacement texture contains no useful fluid inclusions.

The next most abundant texture observed in 52 samples from the Veta Madre is massive silica (quartz) (Fig. 6J). This term refers to quartz veins that have a homogeneous texture, show no banding, fractures or deformation (Dong et al., 1995). This type of silica often appears milky in hand samples, owing to the abundant tiny fluid inclusions in the quartz (< 2 μm). The massive texture represents an original growth feature and can form during slow precipitation at relatively consistent conditions in open space, and is not associated with boiling.

The remaining mineral textures are observed in less than five percent of the samples. The zonal texture was observed in 23 samples. This primary depositional texture is similar to comb texture, but with euhedral quartz crystals that show growth zoning and which are oriented perpendicular to the vein wall (Fig. 7K). The growth zones often contain primary fluid inclusions that record the original depositional conditions. The crustiform texture is a primary depositional texture that has been described by Adams (1920), Lindgren (1933), Bodnar et al., (1985) and Dong et al. (1995). The banding is often symmetrically distributed with respect to both walls (Fig. 7L) and is formed as a result of rapid, episodic fluctuations in temperature, pressure or fluid conditions during

boiling. The original quartz and chalcedony banding is sometimes partially destroyed by recrystallization (Adams, 1920). This type of quartz can contain useful primary and secondary fluid inclusions. Cockade texture is a primary depositional feature that is confined to breccia zones, where rock fragments are surrounded by concentric crusts of quartz (Fig. 7M) (Adams, 1920; Dong et al., 1995). This occurrence of quartz, which is uncommon in the Veta Madre, can contain useful primary and secondary fluid inclusions. Moss texture silica has an origin similar to that of colloform silica, except that it occurs as isolated spheres rather than in continuous bands (Adams, 1920) (Fig. 7N), giving it an appearance that is similar to moss vegetation (Dong et al., 1995). This texture is produced by surface tension affects when silica gel nucleates on impurities suspended in solution. This type of silica contains no useful fluid inclusions. Comb texture quartz (Fig. 7O) is a primary depositional texture that was observed in a few samples. This texture is characterized by coarse, imperfect, euhedral crystals growing into open space perpendicular to the vein walls (Adams, 1920). This type of quartz often contains numerous microfractures that contain secondary fluid inclusions (Bodnar et al., 1985). The ghost-sphere texture is a replacement texture of fine grained, anhedral to spherical crystals that is similar to moss texture when observed under the microscope with uncrossed polars (Adams, 1920). However, under crossed polars this type of silica shows a jigsaw texture (Fig. 7R). This type of silica contains no useful primary fluid inclusions, but secondary inclusions may provide information concerning later conditions.

As noted previously, boiling has been linked to metal deposition in precious metal systems (Buchanan, 1979; Roedder, 1984; Bodnar et al., 1985; Brown, 1986; Simmons and Christenson, 1994; Andre-Mayer et al., 2002; Etoh et al., 2002), and many of the

textures described above are thought to be produced as a result of boiling. At temperatures =340°C, the solubility of quartz decreases with both decreasing pressure and decreasing temperature (Fournier, 1985). Shallow hydrothermal systems such as those associated with epithermal deposits often experience repeated episodes of sealing and fracturing during the lifetime of the system, as evidence by abundant brecciation and broken crystals in epithermal systems. Hydraulic fracturing and the concomitant pressure drop may cause the fluid to boil (or "flash" to steam). When this occurs the temperature also decreases owing the large heat of vaporization of water. As a result, the originally silica-undersaturated fluid may achieve high degrees of silica supersaturation, leading to the precipitation of amorphous silica with a colloform texture. With time, the amorphous silica may recrystallize to chalcedonic silica and/or quartz (Fournier, 1985) to produce many of the textures observed in this study. For example, jigsaw texture quartz, characterized by equant, anhedral interlocking grains is thought to indicate crystallization from gelatinous amorphous silica that precipitated from a solution very supersaturated in silica (Fournier, 1985).

Those textures observed here that are thought to be produced directly by precipitation from supersaturated solutions, or by crystallization of chalcedony or quartz from original amorphous silica, include jigsaw (Fig. 7A), feathery (Fig. 7B), flamboyant (Fig. 7C), plumose (Fig. 7D), colloform (Fig. 7G), colloform banded plumose (Fig. 7H), colloform banded jigsaw (Fig. 7I), crustiform quartz (Fig. 7L), moss (Fig. 7N) and ghost-sphere (Fig. 7R). Similarly, lattice bladed calcite (Fig. 7F), lattice-bladed calcite replaced by quartz (Fig. 7Q) and pseudo-acicular quartz after calcite (Fig. 7P) are also textures associated with boiling fluids. In each sample, the presence of these textures has been

noted and used to infer whether boiling occurred at the sample location at some time during or after deposition of the original material. The number of samples containing each of the textures described here is summarized in Figure 9. A compilation of all data from this study, including sample numbers and locations, assay values for Au, Ag, As, Sb, Cu, Pb and Zn, and which textures were present in each sample is included in Appendix 1.

Fluid inclusions

Petrographic examination of Fluid Inclusion Assemblages (FIAs) can provide evidence concerning the chemical and physical environment of formation of epithermal precious metals deposits (Bodnar et al., 1985; Bodnar, 2003c). As noted by previous workers (Bodnar et al., 1985; Sander and Black, 1988; Dong et al., 1995), some types of silica from the epithermal environment contain no useful fluid inclusions. Thus, primary-appearing fluid inclusions in colloform banded plumose, colloform banded jigsaw, jigsaw and plumose texture silica do not record the conditions of formation because these phases were originally precipitated as amorphous silica or fine-grained chalcedony and have subsequently recrystallized. On the other hand, secondary fluid inclusions trapped along healed fractures in quartz that has recrystallized from amorphous silica or fine-grained chalcedony do record the conditions of this later fracture healing event. In each sample containing these textures, secondary FIAs were monitored to determine if the inclusions showed evidence of boiling.

When fluid inclusions are trapped in a single-phase fluid system, all of the inclusions will show the same phase behavior when observed under the microscope at

room temperature. However, if the inclusions are trapped in a boiling or immiscible fluid system, some inclusions will trap the liquid phase, some will trap the vapor, and some will trap mixtures of the two phases (Bodnar et al., 1985). In each FIA identified as described above, the phase relations of individual inclusions were examined to determine if all the inclusions had the same liquid-to-vapor ratio, or if the inclusions in the FIA showed variable ratios (Fig. 6). Variable liquid-to-vapor ratios may also be produced by necking down of the inclusions *after* a vapor bubble has nucleated in the inclusions. In most cases, it is not possible to distinguish between those FIAs with variable liquid-to-vapor ratios produced by boiling and those produced by necking down. However, we have assumed that if the FIA includes vapor-rich inclusions and liquid-rich inclusions with variable liquid-to-vapor ratios, as well as all-liquid inclusions, that the inclusion phase ratios are the result of necking down or possibly recrystallization of amorphous silica or chalcedony (Sander and Black, 1988), and not the result of boiling (see Goldstein and Reynolds, 1994).

As noted previously, microthermometric analysis was not included in this study. However, because samples were collected over a significant vertical as well as horizontal distance, it was deemed worthwhile to determine if any large gradients in homogenization temperatures are obvious within the study area. Thus, the temperature of homogenization of the inclusions was estimated based on the room temperature phase ratios of the liquid-rich inclusions in the FIAs (Bodnar, 2003c). No obvious homogenization temperature gradients were suggested by the fluid inclusion phase relations, and this is consistent with previous studies by Buchanan (1979) and Mango (1988).

Results and Interpretation

The goal of this study was to examine possible correlations between precious metal mineralization and evidence for boiling along the Veta Madre at Guanajuato, Mexico, and to develop a tool that could be used to evaluate the economic potential of epithermal systems. As noted above, several mineral textures observed in this study, including jigsaw texture silica (Fig. 7A), feathery silica (Fig. 7B), flamboyant texture silica (Fig. 7C), plumose texture silica (Fig. 7D), lattice bladed calcite (Fig. 7F), colloform texture silica (Fig. 7G), colloform banded plumose texture silica (Fig. 7H), colloform banded jigsaw texture silica (Fig. 7I), crustiform quartz (Fig. 7L), moss texture silica (Fig. 7N), pseudo-acicular texture silica after calcite (Fig. 7P), lattice-bladed calcite replaced by quartz (Fig. 6Q), ghost-sphere texture silica (Fig. 7R), suggest rapid precipitation as a result of boiling. In addition, the presence of coexisting liquid-rich and vapor-rich fluid inclusions in the same FIA indicates that the inclusions were trapped in a boiling fluid.

For each of the 855 samples examined, a numerical value was assigned for each mineral texture and fluid inclusion feature described above. A value of 0 (zero) was assigned if a given feature was not observed during petrographic examination of the sample, and a value of 1 (one) was assigned if the feature was observed. The number of observations for each of the boiling features is summarized in Figure 9. Jigsaw texture quartz was observed in nearly every sample (752 of 855 samples). Plumose texture quartz, also referred to as feathery or flamboyant texture quartz in the literature, occurs in 549 samples, colloform texture silica, including colloform banded plumose and colloform

banded jigsaw textures, was observed in 193 samples, and lattice bladed calcite + lattice bladed calcite replaced by quartz + acicular calcite replaced by quartz was observed in 120 samples. Fluid inclusion assemblages containing coexisting liquid-rich and vapor-rich fluid inclusions were observed in 193 samples (Fig. 9).

For each of the textures described above, the average Au and Ag grade of samples in which the feature is present, and the average Au and Ag grade for samples in which that feature is absent, have been calculated and the results are shown on Figures 10 and 11. The average grade of Au is higher in samples in which the boiling feature is present, compared to samples for which it is absent, except for the cockade texture silica (Fig. 10). Also, the most dramatic difference in grade between the presence or absence of that feature is colloform texture (1.1 ppm Au versus 0.2 ppm Au). And, the average grade is lower in samples that exhibit non-boiling textures, including massive, zonal and comb texture quartz and rhombic calcite.

The average grade of silver is higher in samples in which a feature indicative of boiling is present for all features except for the jigsaw texture quartz. The average Ag grade is lower in samples that show mineral textures that are indicative of slow crystal growth (non-boiling), including massive, zonal, cockade and comb texture quartz – the lone exception is rhombic calcite, which is not thought to be associated with boiling. Features that show the most dramatic difference in Ag grade between the presence or absence of that feature are colloform texture silica (178.8 ppm Ag versus 17.2 ppm Ag) and bladed/platy calcite (128.4 ppm Ag versus 47.5 ppm Ag).

There is no significant difference in average grade of samples containing both liquid-rich and vapor-rich fluid inclusions, compared to those in which fluid inclusion

evidence for boiling is absent. The Au grades are essentially identical (0.4 ppm Au) in samples containing boiling FIAs and those in which they are absent (Fig. 10). The Ag grade is slightly elevated in samples containing coexisting liquid-rich and vapor-rich fluid inclusions, compared to those in which fluid inclusion evidence for boiling is absent (67.1 ppm Ag versus 49.4 ppm Ag; Fig 11).

Data shown on Figures 10 and 11 were evaluated using the t-test to assess whether the average grades (means)for samples in which a feature is present are statistically different from those in which the feature is absent. Differences between the presence or absence of a feature indicative for boiling are statistically different at the 95% confidence level ($p<0.05$) for all features except jigsaw texture silica ($p<0.10$) and fluid inclusions ($p<0.25$) for silver, and for fluid inclusions ($p<0.10$) (Fig. 12). For comparison, the distribution of grades for samples in which massive quartz (a non-boiling texture) is present and absent is shown on Figure 12. Note that the sample groups are statistically different for Au, but that samples containing massive quartz are lower than those in which it is absent. This is consistent with the observation that Au (and Ag) is closely associated with textures indicative of boiling and is not related to non-boiling textures.

The textural and fluid inclusion data obtained in this study were analyzed using the binary classifier within the statistical software package SPSS Clementine. The binary classifier builds 10 different statistical models and evaluates the performance of each model (Fig. 13a, b). The Au and Ag grades show a log normal distribution based on application of the Shapiro-Wilks test for normality (Fig. 14a. b). Our goal was to develop and test models that could distinguish between samples with high ore grades (=1 ppm Au

or =100 ppm Ag) and those with lower grades. Each sample was assigned a label that identified whether the concentration was above or below these thresholds. Of the 694 samples for which we had Au and Ag assay data, only about 6% of the observations were found to be high grade (=1 ppm Au or =100 ppm Ag) for either gold or silver.

In order to build an unbiased statistical model, the number of observations was balanced via random sampling to contain an approximately equal number of high and low grade samples. If an equal number of high and low grade samples was not selected to develop the model, the model would tend to over-predict the grade with a higher frequency in the sample population. For Au, after balancing, 78 samples were selected to build the models (36 had Au =1 ppm and 42>1 ppm). Similarly, for Ag, 77 samples were selected to build the models - 38 samples had >100 ppm Ag and 39 <100 ppm Ag.

After balancing, the dataset was split into a training dataset (70% of the observations) and testing dataset (30% of the observations). The software iteratively builds and evaluates the predictive models and ranks the resulting models based on accuracy, i.e., the proportion of correct predictions. The models that showed the highest "profit" or greatest accuracy for both Au and Ag were the neural network, the C5 decision tree and Quest decision tree models, all of which predicted the correct results in about 70-75% of the tests. For both Ag and Au, most other models showed significantly lower accuracy.

The binary classifier model building and testing software also provides information on the relative importance of each of the variables included in the model. For both Au and Ag, the presence of colloform silica texture was the variable with the greatest importance, i.e., colloform texture silica has the greatest predictive power to

distinguish between higher grade samples and lower grade samples. For Au, the second most important variable was bladed/platy calcite (Fig. 15a), and for Ag coexisting liquid-rich and vapor-rich fluid inclusions showed the second highest importance (Fig. 15b).

Application in Exploration for Epithermal Precious Metal Deposits

The results of the is study may be used in exploration for epithermal precious metals deposits, both at the "grass roots" or early exploration stage to find new deposits, and during mine development and exploration in existing deposits. The applications described here are based on the assumption that precious metal mineralization and boiling are genetically related. Moreover, it must be emphasized that not all hydrothermal fluids in the epithermal environment contain Au and/or Ag – thus some systems may show significant boiling textures but contain no Au or Ag mineralization.

The feature that is most closely related to higher Au and Ag grades in the Veta Madre is colloform texture silica. This texture is often easily recognizable in outcrop and hand sample, as well as during normal petrography. Lattice bladed or platy calcite and plumose texture silica are also closely associated with high grade samples in the Veta Madre. While lattice bladed calcite is recognizable in hand sample, it may be necessary to examine samples in crossed polars under the microscope to reveal the plumose texture. Fluid inclusions show only a poor correlation with higher Au and Ag grades at Guanajuato. This lack of correlation reflects the fact that inclusions are not trapped during precipitation of the amorphous silica phases and inclusions that are trapped during precipitation of lattice bladed calcite are often destroyed when the calcite is replaced by quartz.

Most samples collected from the Veta Madre in this study show some evidence of boiling (>750 out of 855 samples). Most of the samples that do not show evidence of boiling consist of only rhombic calcite which is not thought to be precipitated during boiling. With distance away from the Veta Madre, the Ag and Au grades drop of drastically (Fig. 16 B, C). The only feature that is recognized in 4 samples collected along a traverse perpendicular to the vein is jigsaw texture silica (Fig. 16A). The rapid drop-off in boiling intensity (and Ag and Au grades) with distance from the mineralized vein has both advantages and disadvantages for exploration. The disadvantage is that the target area that can be defined using these features has relatively small lateral extent on the surface. Conversely, if an exploration sample collected from the surface contains good evidence for boiling, it is likely that this represents the heart of the system and defines the location where mineralization should occur if the system is mineralized.

As noted earlier, and as observed in modern geothermal systems, once boiling begins at depth it usually continues to the surface. Additionally, the best gold grades occur at the base of the boiling zone where upward migrating fluids begin to boil. Therefore, good evidence of boiling in surface samples indicates that the base of the boiling zone where precious metal mineralization is mostly likely to occur, is beneath the present surface and should be given high priority for drilling to explore the subsurface, even if precious metal grades in the surface samples are poor. At Guanajuato, an angled drill hole from the surface into the Veta Madre showed a systematic increase in boiling intensity factor as the vein was approached (Fig. 16D), even though the metal grades in the drill core were well below economic values.

It is necessary to have a well-designed mine plan to maximize production and profit in an operating mine, and this requires information on the potential for additional resources in rock outside of current mining activities. At Guanajuato the proportion of samples showing good evidence of boiling increases with depth to the deepest levels of current mining activities and beyond in drill core (Fig. 17). This suggests that the bottom of the boiling horizon is at some depth greater than that explored by mining and drilling, and that additional precious metal resources are likely to be encountered in the future as deeper levels of the Veta Madre system are explored and developed.

References

Abeyta, R. L., (2003) Epithermal gold mineralization of the San Nicholas Vein, El Cubo Mine, Guanajuato, Mexico: Trace element distribution, fluid inclusion microthermometry and gas chemistry. Unpublished Master's thesis, New Mexico Institute of Mining and Technology, Socorro, NM, 129 pp.

Adams, S. F., (1920) A microscopic study of vein quartz. Economic Geology, 15, 8, p. 623-664.

Albinson, T., Norman, D. I., Cole, D., and Chomiak B., (2001) Controls on formation of low-sulfidation epithermal deposits in Mexico: Constraints from fluid inclusion and stable isotope data. Society of Economic Geologists Special Publication 8, p. 1-32.

Andre-Mayer, A.-S., Leroy, J. L., Bailly, L., Chauvet, A., Marcoux, E., Grancea, L., Llosa, F., and Rosas, J., (2002) Boiling and vertical mineralization zoning; a case study from the Apacheta low-sulfidation epithermal gold-silver deposit, southern Peru. Mineralium Deposita, 37, 5, p. 452-464.

Aranda-Gómez, J. J., Godchaux, M. M., Aguirre-Díaz, G. J., Bonnichsen, B., Martínez-Reyes, J., (2003) Three superimposed volcanic arcs in the southern Cordillera—from the Early Cretaceous to the Miocene, Guanajuato, Mexico. In: Geologic Transects Across Cordilleran Mexico, Guidebook for Field Trips of the 99th Annual Meeting of the Cordilleran Section of the Geological Society of America, Mexico, D. F., April 5–8, 2003. Universidad Nacional Autónoma de México, Instituto de Geología, Publicación Especial 1, Field trip 6, p. 121–168.

Bodnar RJ (1983) A method of calculating fluid inclusion volumes based on vapor bubble diameters and P-V-T-X properties of inclusion fluids. Economic Geology, 78, 535-542.

Bodnar, R. J., (2003a) Introduction to fluid inclusions, *in* Samson, I., Anderson, A., and Marshall, D., eds., Fluid Inclusions: Analysis and interpretation: Mineralogical Association of Canada, Short Course 32, p. 1–8.

Bodnar, R. J., (2003b) Reequilibration of fluid inclusions, *in* Samson, I., Anderson, A., and Marshall, D., eds., Fluid inclusions: Analysis and interpretation: Mineralogical Association of Canada, Short Course 32, p. 213–230.

Bodnar RJ (2003c) Introduction to aqueous fluid systems. *In* I. Samson, A. Anderson, & D. Marshall, eds. Fluid Inclusions: Analysis and Interpretation. *Mineral. Assoc. Canada, Short Course* 32, 81-99.

Bodnar, R. J., Reynolds, T. J., and Kuehn, C. A., (1985) Fluid-inclusion systematics in epithermal systems. Reviews in Economic Geology, 2, p. 73-97.

Brown, K. L., (1986) Gold deposition from geothermal discharges in New Zealand. Economic Geology, 81, 4, p. 997-983.

Buchanan, L. J., (1979) The Las Torres Mines, Guanajuato, Mexico: Ore controls of a fossil geothermal system. Unpublished Ph. D. dissertation, Colorado School of Mines, Golden, Colorado, 138 pp.

Buchanan, L. J., (1980) Ore controls of vertically stacked deposits, Guanajuato, Mexico. American Institute of Mining Engineers, Preprint 80-82, p. 26.

Buchanan, L. J., (1981) Precious metal deposits associated with volcanic environments in the Southwest. Arizona Geological Society Digest 14, p. 237-262.

Casadevall, T., and Ohmoto, H., (1977) Sunnyside Mine, Eureka mining district, San Juan County, Colorado: Geochemistry of gold and base metal ore deposition in a volcanic environment. Economic Geology, 72, 7, p. 1285-1320.

Church, J. A., (1907) The Mines of La Luz, Guanajuato, Mexico II. The engineering and mining journal, p. 105-110.

Clark, K. F., Foster, C. T., and Damon, P. E., (1982) Cenozoic mineral deposits and subduction-related magmatic arcs in Mexico. GSA Bulletin, 93, 6, p. 533-544.

Cline, J. S., Bodnar, R. J., and Rimstidt, J. D., (1992) Numerical simulation of fluid flow and silica transport and deposition in boiling hydrothermal solutions: Application to epithermal gold deposits. Journal of Geophysical Research, 97, B6, p. 9085-9103.

Cornelius, K. D., (1964) Geology of the footwall formations of the Veta Madre, Guanajuato Mining District, Guanajuato, Mexico. Unpublished Master's thesis, University of Arizona, Tucson, AZ, 42 pp.

Dávila, V. M., and Martínez Reyes, J., (1987) Un edad Cretacica para las rocas basales de la Sierra de Guanajuato. Universidad Nacional Autonoma de Mexico. April 28-30, Resumen, p. 19-20.

Dong, G., Morrison, G., and Jaireth, S., (1995) Quartz textures in epithermal veins, Queensland; classification, origin and implication. Economic Geology, 90, 6, p. 1841-1856.

Echegoyen-Sanchez, J., (1964) Algunos datos sobre la mineralizacion de la Veta Madre de Guanajuato. In I er Seminario sobre Exploracion Geologico-Minera, Mem. p. 134-149.

Edwards , J. D., (1955) Studies of some early Tertiary red conglomerates of central Mexico. U. S. Geological Survey Professional Paper. P0264-H. 185 pp.

Etoh, J., Izawa, E., Watanabe, K., Taguchi, S., and Sekine, R., (2002) Bladed quartz and its relationship to gold mineralization in the Hishikari low-sulfidation epithermal gold deposit, Japan. Economic Geology, 97, 8, p. 1841-1851.

Fournier, R. O., (1985) The behavior of silica in hydrothermal solutions. Reviews in Economic Geology, 2, p. 45-61.

Girnius, R., (1993) Deposition of the upper ore in the El Cubo mine, Guanajuato mining district, Mexico. Unpublished Senior's thesis, Dartmouth College, Hanover, NH, 21 pp.

Godchaux, M. M., Bonnichsen, B., Aguirre Diaz, G. de J., Aranda Gomez, J. J., Rangel Solis, G., and Anonymous., (2003) Volcanological and tectonic evolution of a complex Oligocene caldera system, Guanajuato mining district, central Mexico. Geological Society of America, Abstracts with Programs, 35, 4, p. 8.

Goldstein, R.H., and Reynolds, T.J., (1994) Systematics of fluid inclusions in diagenetic minerals: Society for Sedimentary Geology Short Course 31, 199pp.

Gross, W. H., (1975) New ore discovery and source of silver-gold veins, Guanajuato, Mexico. Economic Geology, 70, 7, p. 1175-1189.

Guiza, R., (1949) Estudio geologico del distrito minero de Guanajuato, Gto. (Zona de la Veta Madre). Mexico Inst. Nac. Inv. Rec. Miner 22 p.

Gunnarsson, I. and Arnórsson, S., (2000) Amorphous silica solubility and the thermodynamic properties of $H_4SiO_4^0$ in the range 0° to 350°C at P_{sat}. Geochimica et Cosmochimica Acta, 64, 13, 2295-2307.

Hedenquist, J. W., Arribas R, A., and Gonzalez-Urien, E., (2000) Exploration for epithermal gold deposits. Reviews in Economic Geology, 13, p. 245-277.
Helgeson, H. C., (1969) Thermodynamics of hydrothermal systems at elevated temperatures and pressures. American Journal of Science, 267, 7, 729-804.
Henley, R. W., and Brown, K. L., (1985) A practical guide to the thermodynamics of geothermal fluids and hydrothermal ore deposits. Reviews in Economic Geology, 2, p. 25-44.
Henley, R. W., and Hughes, G. O., (2000) Underground fumaroles: "Excess heat" effects in vein formation. Economic Geology, 95, 3, p. 453-466.
Kamilli, R. J. and Ohmoto, H., (1977) Paragenesis, zoning, fluid inclusion, and isotopic studies of the Finlandia Vein, Colqui District, central Peru. Economic Geology, 72, 6, p. 950-982.
Lindgren, W., and Knowlton, F. H., (1896) The gold-quartz veins of Nevada City and Grass Valley districts, California. United States Geological Survey Annual Report, 17, Part 2, p. 1-262.
Lindgren, W., (1933) Mineral deposits, 4th edition, New York, McGraw-Hill, 930 pp.
Mango, H., (1988) A fluid inclusion and isotopic study of the Las Rayas Ag-Au-Pb-Cu mine.Unpublished Master's thesis, Dartmouth College, Hanover, NH, 109 pp.
Mango, H., Zantop, H., and Oreskes. N., (1991) A fluid inclusion and isotope study of the Rayas Ag-Au-Cu-Pb-Zn mine, Guanajuato, Mexico. Economic Geology, 86, 7, p. 1554-1561.
Pokrovski, G. S., Borisova, Yu. A., and Harrichoury, J.-C., (2008) The effect of sulfur on vapor-liquid fractionation of metals in hydrothermal systems. Earth and Planetary Science Letters 266 (3-4), p. 345-362.
Randall, J. A., Saldana, E. A., and Clark, K. F., (1994) Exploration in a volcano-plutonic center at Guanajuato, Mexico. Economic Geology, 89, 8, p. 1722-1751.
Roedder, E., (1984) Fluid inclusions. Reviews in Mineralogy, 12, 644 pp.
Roedder, E. and Bodnar, R. J., (1997) Fluid Inclusion Studies of Hydrothermal Ore Deposits. *in* Geochemistry of Hydrothermal Ore Deposits, 3rd ed., H. L. Barnes, ed., Wiley & Sons, Inc, New York, 657-698.
Rogers, A. F., (1918) The occurrence of cristobalite in California. American Journal of Science, 45, 267, p. 222-226.
Sander, M. V. and Black, J. E., (1988) Crystallization and recrystallization of growth-zoned vein quartz crystals from epithermal systems; implications for fluid inclusion studies. Economic Geology, 83, 5, p. 1052-1060.
Shenberger, D. M. and Barnes, H. L., (1989) Solubility of gold in aqueous sulfide solutions from 150 to 350°C. Geochimica et Cosmochimica Acta, 53, 2, 269-278.
Sillitoe, R.H., and Hedenquist, J.W., (2003) Linkages between volcanotectonic settings, ore-fluid compositions, and epithermal precious-metal deposits, *in* Simmons, S.F., Graham, I., eds., Volcanic, geothermal, and ore-forming fluids: Rulers and witnesses of processes within the earth. Society of Economic Geologists Special Publication 10; p. 315-343.
Simmons, S. F. and Brown, K. L., (2008) Precious metals in modern hydrothermal solutions and implications for the formation of epithermal ore deposits. Society of Economic Geologists Newsletter, Number 72, January, 2008, published by the Society of Economic Geologists, Littleton, Colorado, pp. 1, 9-12.

Simmons, S. F. and Christenson, B. W., (1994) Origins of calcite in a boiling geothermal system. American Journal of Science, 294, 3, p. 361-400.
Simmons, S. F., White, N. C., and John, D. A., (2005) Geological characteristics of epithermal precious and base metal deposits. Economic Geology 100th Anniversary Volume, Economic Geology: One Hundredth Anniversary Volume, 1905-2005, p. 485-522.
Stewart, M., (2006) Geology of Guanajuato and La Luz Areas, Mexico. Unpublished geologic map.
Taylor, P. S., (1971) Mineral variations in the silver veins of Guanajuato, Mexico., Unpublished Ph. D. dissertation, Dartmouth College, Hanover, NH, 136 pp.
Ulrich, M.R., and Bodnar, R.J., (1988) Systematics of stretching of fluid inclusions. II. Barite at one atmosphere confining pressure. Economic Geology, v. 83, p. 1037-1046.
Van den Kerkhof, A. M. and Hein, U. F., (2001) Fluid inclusion petrography. Lithos, 55, 1-4, p. 27-47.
Vikre, P. G., (1985) Precious metal vein systems in the National District, Humboldt County, Nevada. Economic Geology, 80, 2, p. 360-393.
Wandke, A. and Martinez, J., (1928) The Guanajuato mining district, Guanajuato, Mexico. Economic Geology, 23, 1, p. 1-44.
Wilson, I. F., Milton, C., and Houston, J. R., (1950) A mineralogical study of Guanajuato, Mexico, silver-gold ores, U.S. Geological Survey Report No. IWM-269, U.S. Geological Survey. unpaginated.

Location	Homogenization temperature (Th)	% wt. NaCl	Deeper sample collection, elevation (meters)	Boiling	Study by:
Rayas Mine, Cata Mine	215 ºC to 299 ºC	no record	1820	none record	Wilson, et al., (1950)
Rayas Mine	230 to 305 ºC	0.5 to 3.4	1675	none evidence	Mango, H. (1988) Mango, et al. (1991)
Las Torres, Veta Madre, Rayas Mine	231 ºC to over 360 ºC	no record	1705	evidence	Buchanan (1979)
Veta Madre, Sierra System	260 ºC to 320 ºC	no record	1700	none record	Gross, W. H. (1975)
Cata Mine	220 ºC to 235 ºC	1.6 to 5	2270	evidence	Girnius, R. (1993)
Cata Mine	172 ºC to 282 ºC	0 to 2.95	2100	evidence	Abeyta, R. L. (2003)

Table 1.

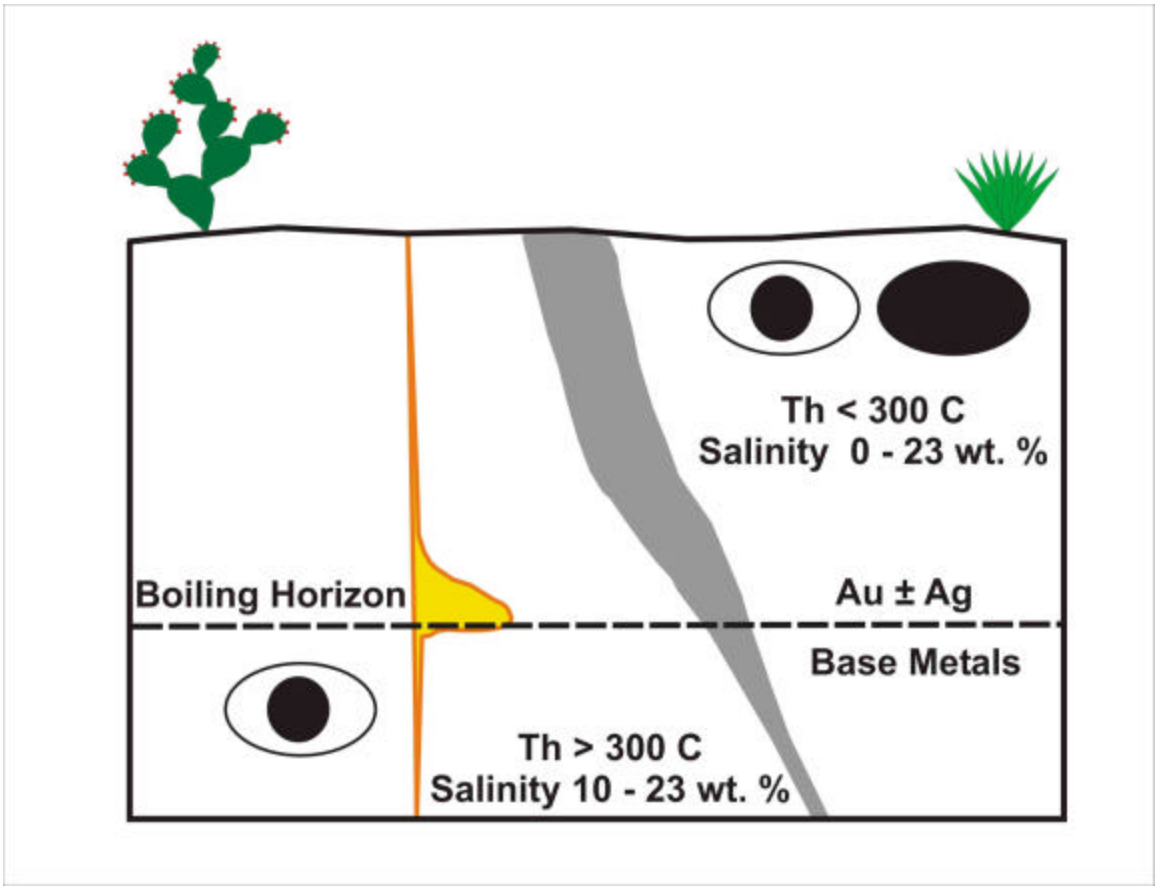
Th < 300 C
Salinity 0 - 23 wt. %
Boiling Horizon
Au ± Ag
Base Metals
Th > 300 C
Salinity 10 - 23 wt. %
Figure 1.

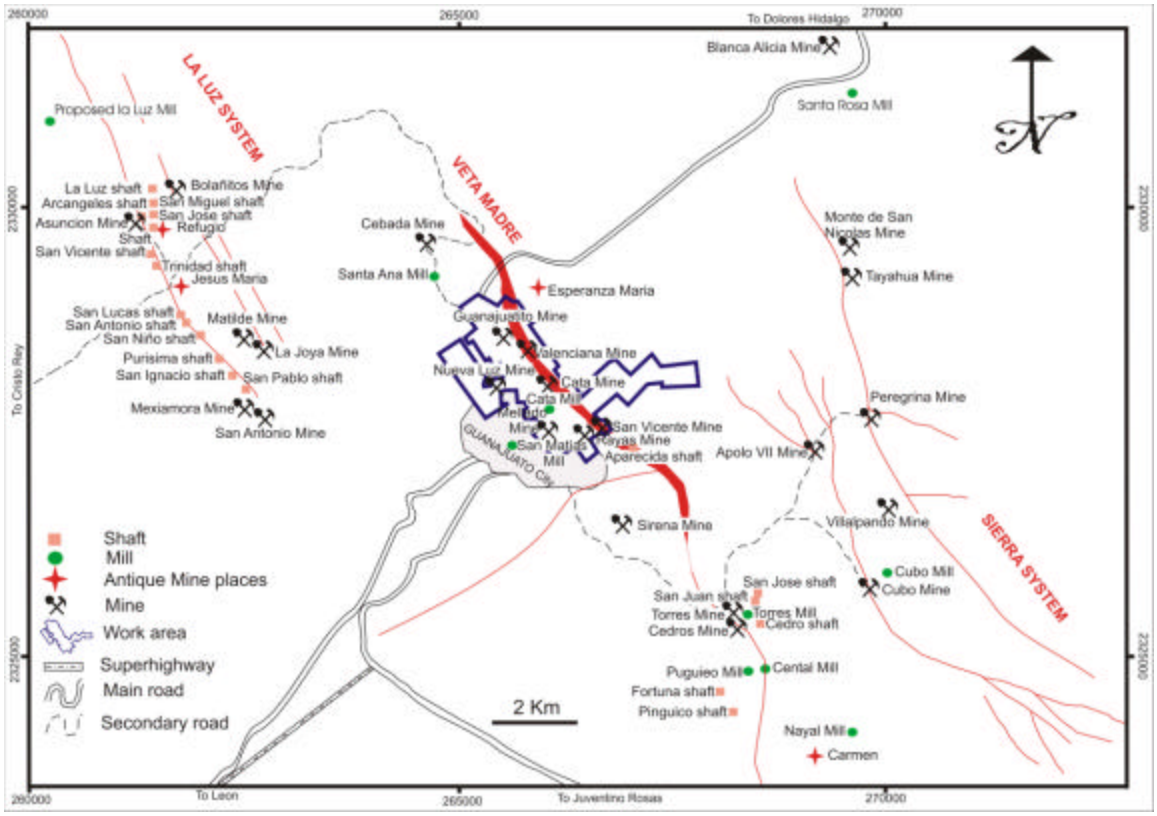
260000
265000
270000
To Dolores Hidalgo
Blanca Alicia Mine
Santa Rosa Mill
LA LUZ SYSTEM
Proposed la Luz Mill
VETA MADRE
La Luz shaft
Bolañitos Mine
Arcangeles shaft
San Miguel shaft
San Jose shaft
Asuncion Mine
Refugio Shaft
San Vicente shaft
Trinidad shaft
Jesus Maria
Cebada Mine
Santa Ana Mill
Esperanza Maria
Guanajuato Mine
Monte de San Nicolas Mine
Tayahua Mine
San Lucas shaft
San Antonio shaft
San Niño shaft
Matilde Mine
La Joya Mine
Purisima shaft
San Ignacio shaft
San Pablo shaft
Mexiamora Mine
San Antonio Mine
Valenciana Mine
Nueva Luz Mine
Cata Mine
Cata Mill
Melladito Mine
San Vicente Mine
Rayas Mine
Aparecida shaft
San Matias Mill
GUANAJUATO Cia.
Peregrina Mine
Apolo VII Mine
Sirena Mine
Villalpando Mine
SIERRA SYSTEM
Cubo Mill
Cubo Mine
San Jose shaft
San Juan shaft
Torres Mine
Torres Mill
Cedro shaft
Cedros Mine
Puguieo Mill
Cental Mill
Fortuna shaft
Pinguico shaft
Nayal Mill
Carmen
2 Km
To Cristo Rey
2330000
2325000
2330000
2325000
Shaft
Mill
Antique Mine places
Mine
Work area
Superhighway
Main road
Secondary road
260000
To Leon
265000
To Juventino Rosas
270000
Figure 2

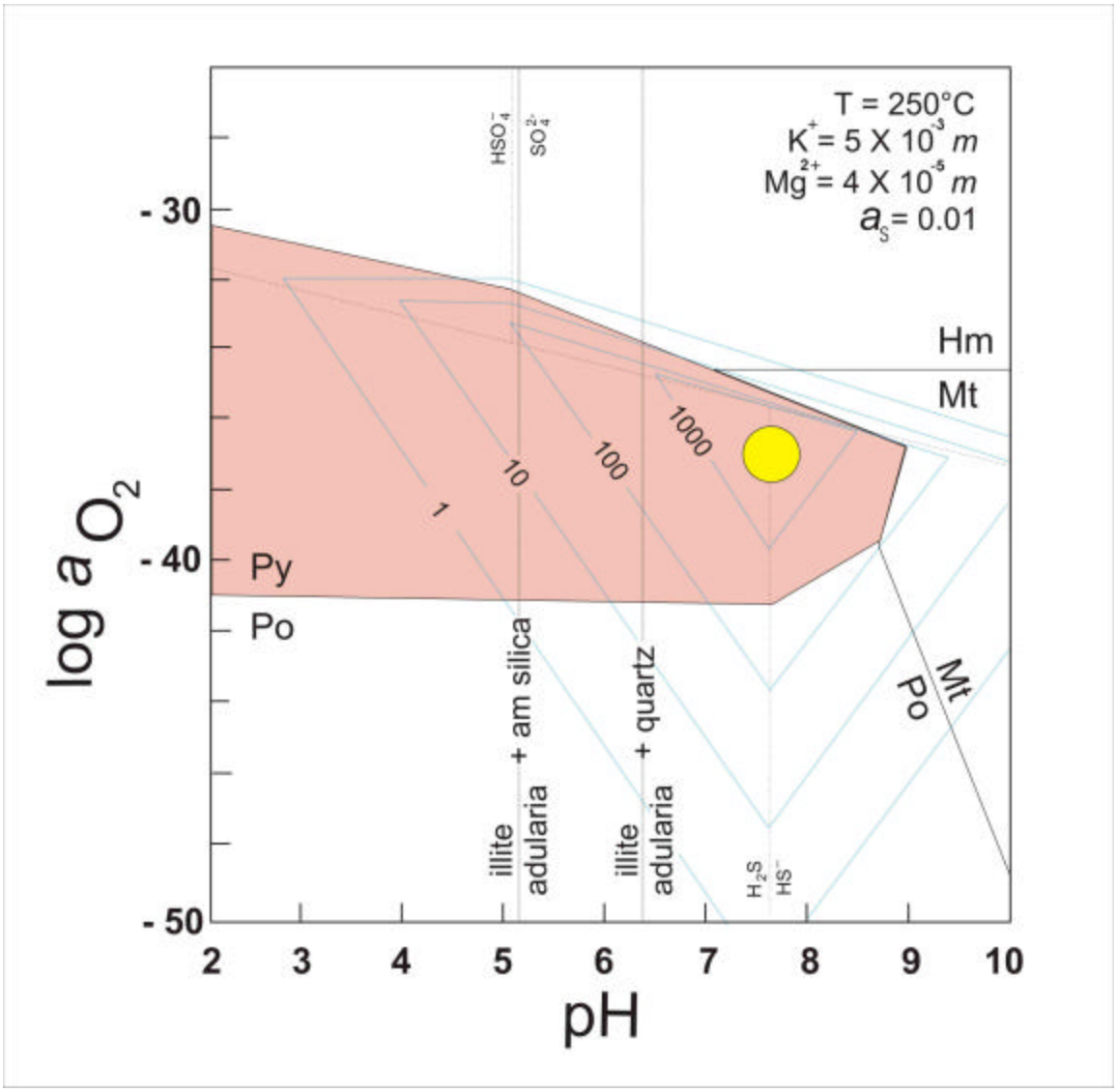
T = 250°C
K+ = 5 X 10-3 m
Mg2+ = 4 X 10-5 m
aS = 0.01
HSO4-
SO42-
Hm
Mt
1000
100
10
1
Py
Po
+ am silica
illite
adularia
+ quartz
illite
adularia
H2S
HS-
Po
Mt
log aO2
- 30
- 40
- 50
2
3
4
5
6
7
8
9
10
pH

Figure 3

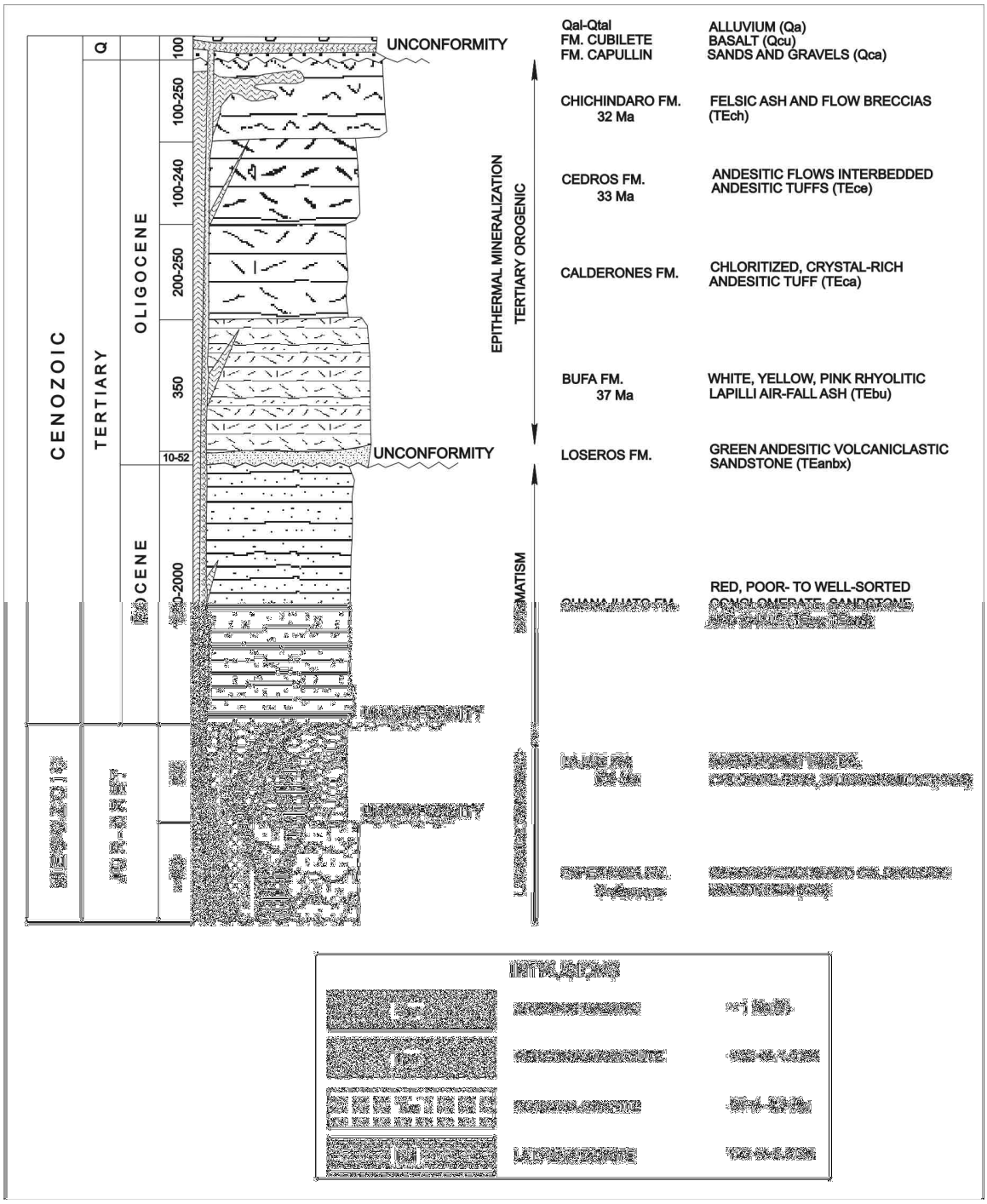
CENOZOIC
TERTIARY
Q
OLIGOCENE
EOCENE
100
100-250
100-240
200-250
350
10-52
1000-2000
UNCONFORMITY
UNCONFORMITY
EPITHERMAL MINERALIZATION
TERTIARY OROGENIC
MATISM
Qal-Qtal
FM. CUBILETE
FM. CAPULLIN
ALLUVIUM (Qa)
BASALT (Qcu)
SANDS AND GRAVELS (Qca)
CHICHINDARO FM.
32 Ma
FELSIC ASH AND FLOW BRECCIAS
(TEch)
CEDROS FM.
33 Ma
ANDESITIC FLOWS INTERBEDDED
ANDESITIC TUFFS (TEce)
CALDERONES FM.
CHLORITIZED, CRYSTAL-RICH
ANDESITIC TUFF (TEca)
BUFA FM.
37 Ma
WHITE, YELLOW, PINK RHYOLITIC
LAPILLI AIR-FALL ASH (TEbu)
LOSEROS FM.
GREEN ANDESITIC VOLCANICLASTIC
SANDSTONE (TEanbx)
RED, POOR- TO WELL-SORTED

Figure 4

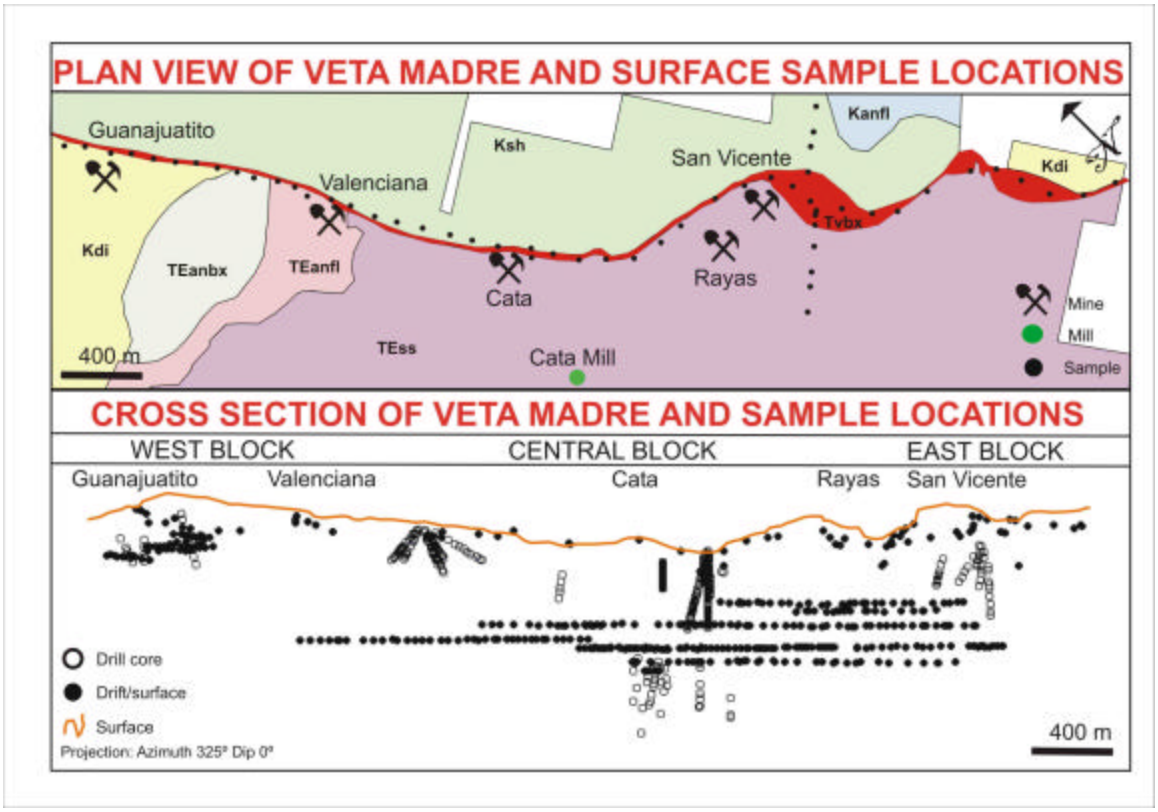
PLAN VIEW OF VETA MADRE AND SURFACE SAMPLE LOCATIONS
Guanajuatito
Valenciana
Ksh
San Vicente
Kanfl
Kdi
Tvbx
Kdi
TEanbx
TEanfl
Cata
Rayas
Mine
Mill
Sample
400 m
TEss
Cata Mill
CROSS SECTION OF VETA MADRE AND SAMPLE LOCATIONS
WEST BLOCK
CENTRAL BLOCK
EAST BLOCK
Guanajuatito
Valenciana
Cata
Rayas
San Vicente
Drill core
Drift/surface
Surface
Projection: Azimuth 325° Dip 0°
400 m
Figure 5

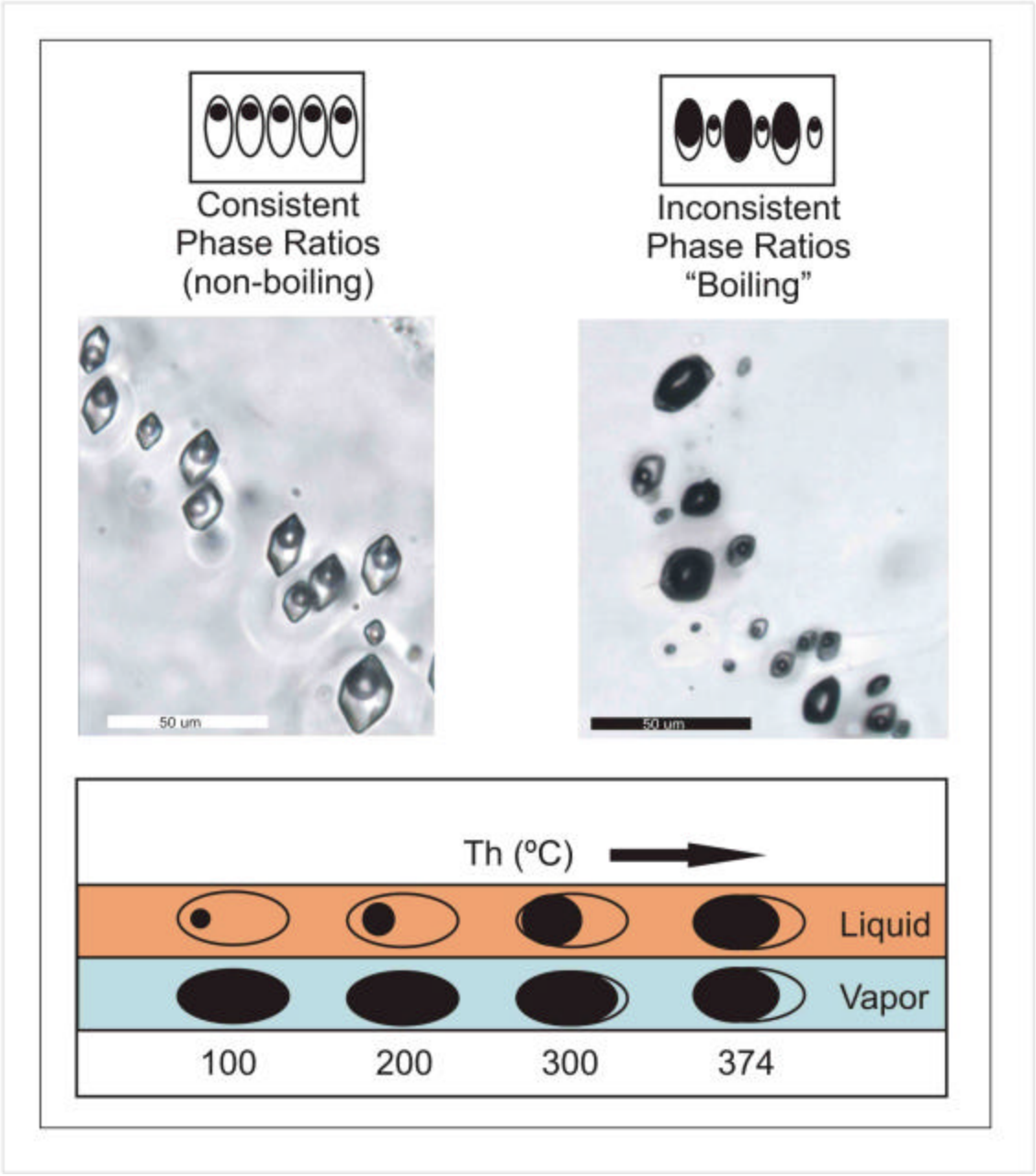
Consistent
Phase Ratios
(non-boiling)
Inconsistent
Phase Ratios
"Boiling"
50 um
50 um
Th (°C)
Liquid
Vapor
100
200
300
374

Figure 6

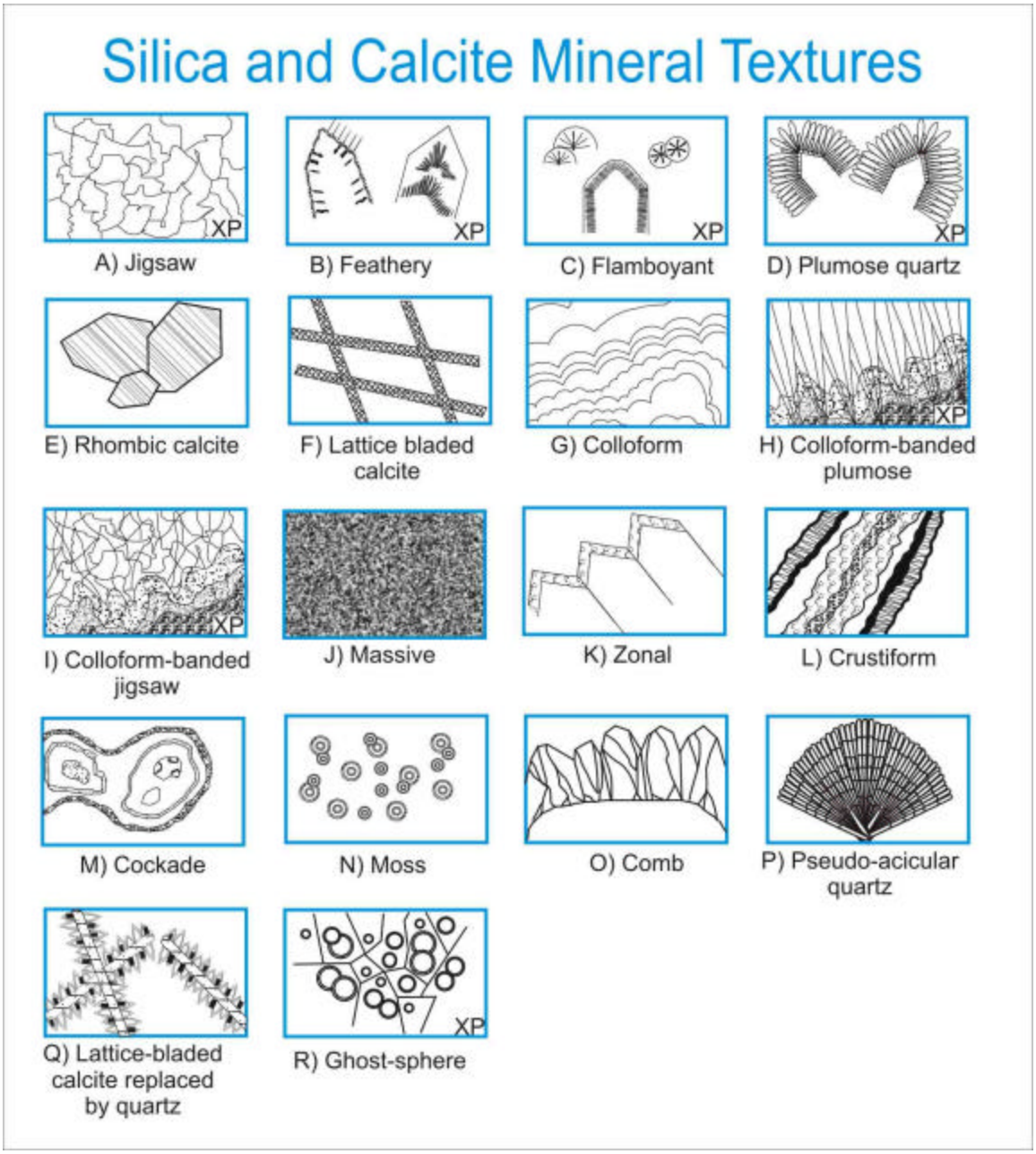
Silica and Calcite Mineral Textures
XP
A) Jigsaw
XP
B) Feathery
XP
C) Flamboyant
XP
D) Plumose quartz
E) Rhombic calcite
F) Lattice bladed calcite
G) Colloform
XP
H) Colloform-banded plumose
XP
I) Colloform-banded jigsaw
J) Massive
K) Zonal
L) Crustiform
M) Cockade
N) Moss
O) Comb
P) Pseudo-acicular quartz
Q) Lattice-bladed calcite replaced by quartz
XP
R) Ghost-sphere

Figure 7

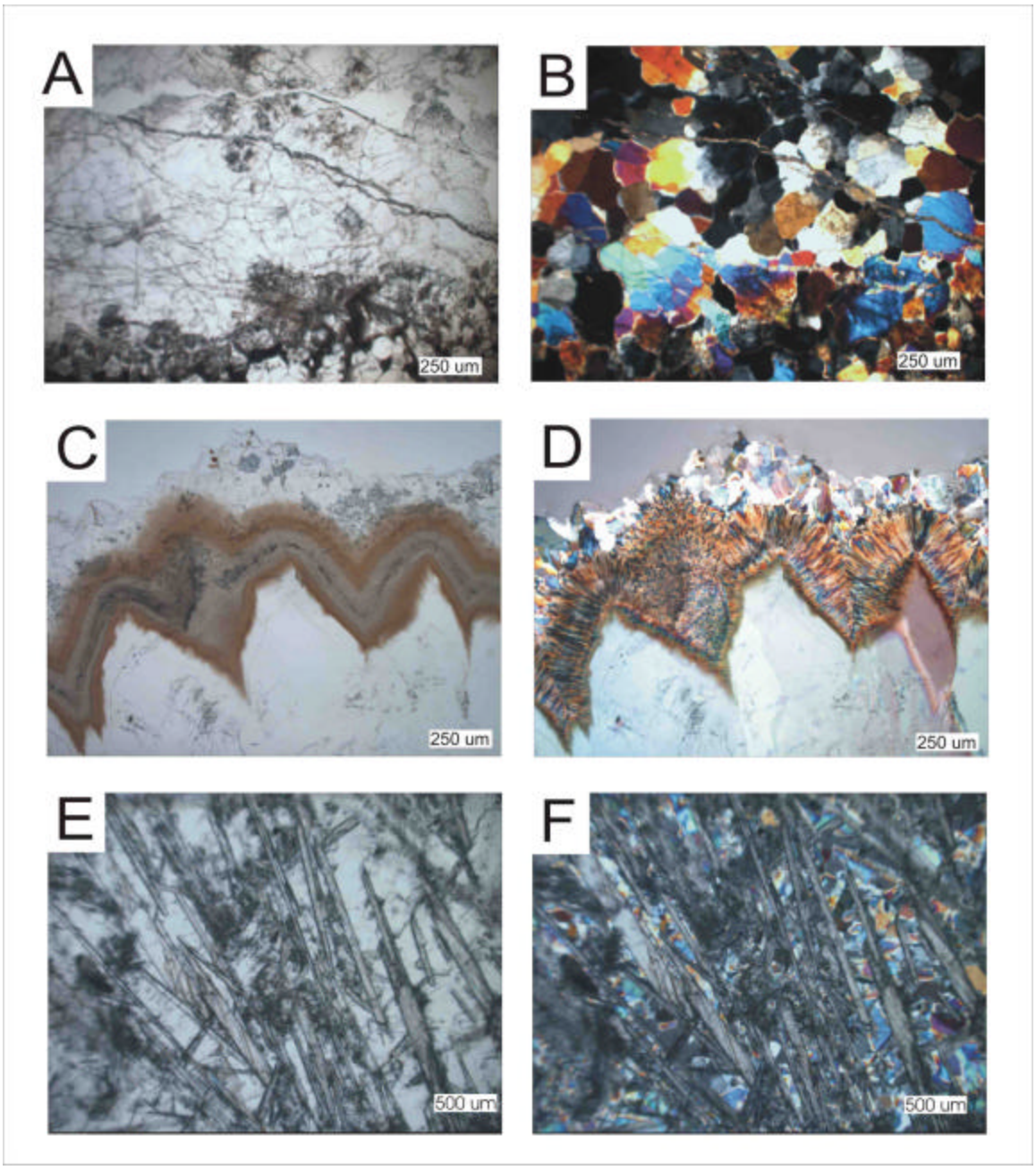

Figure 8

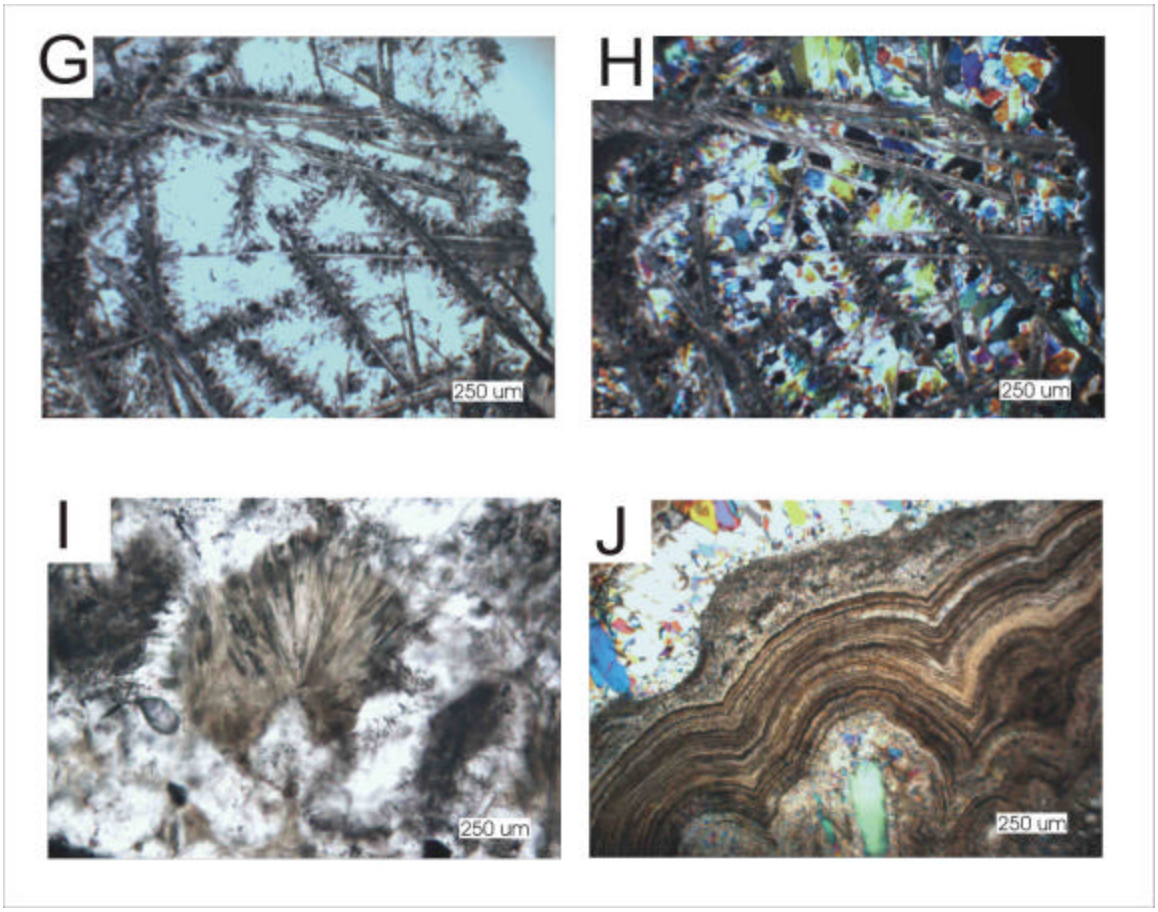

Figure 8

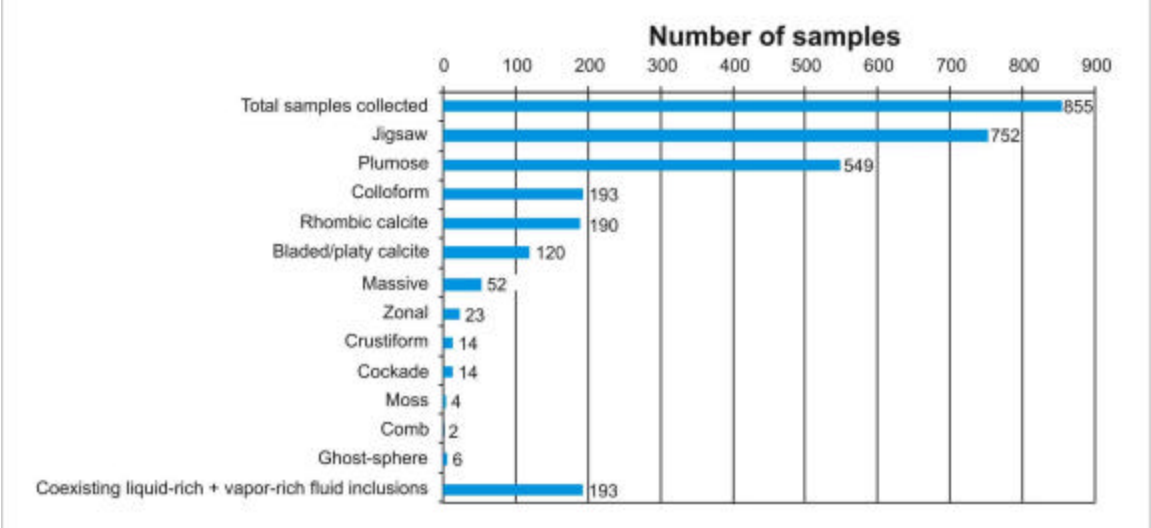
Number of samples
0
100
200
300
400
500
600
700
800
900
Total samples collected
855
Jigsaw
752
Plumose
549
Colloform
193
Rhombic calcite
190
Bladed/platy calcite
120
Massive
52
Zonal
23
Crustiform
14
Cockade
14
Moss
4
Comb
2
Ghost-sphere
6
Coexisting liquid-rich + vapor-rich fluid inclusions
193
Figure 9

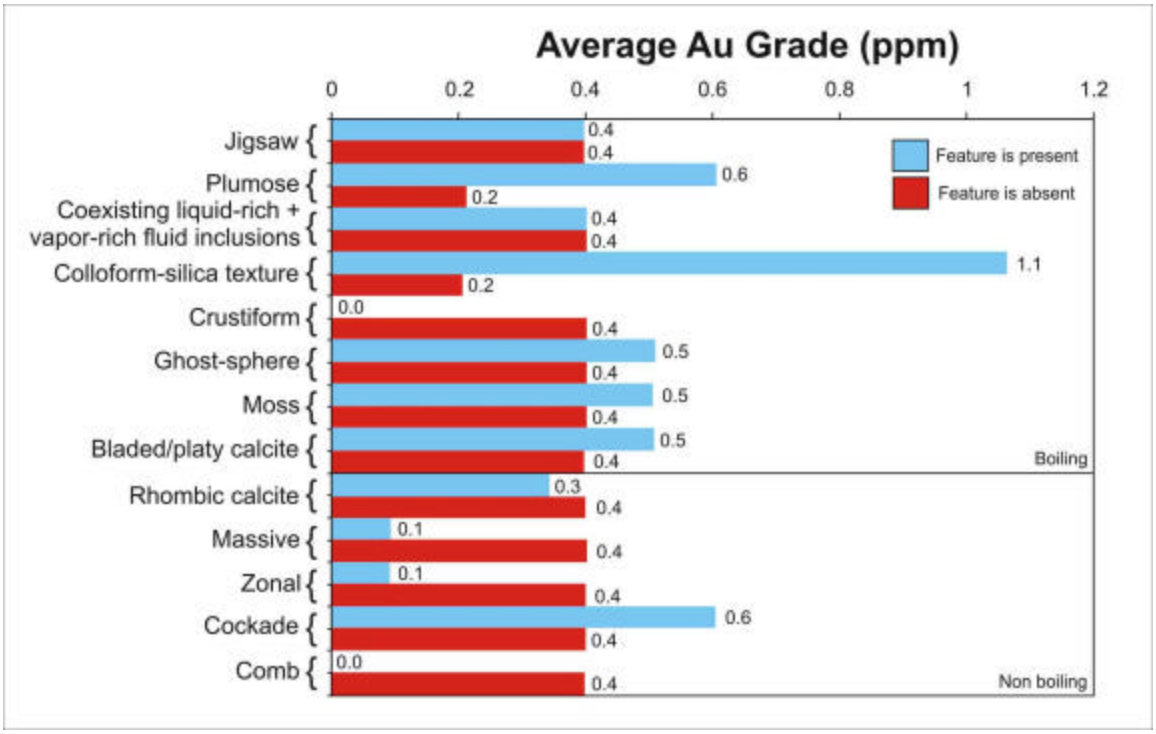
Average Au Grade (ppm)
0
0.2
0.4
0.6
0.8
1
1.2
Jigsaw
Plumose
Coexisting liquid-rich + vapor-rich fluid inclusions
Colloform-silica texture
Crustiform
Ghost-sphere
Moss
Bladed/platy calcite
Rhombic calcite
Massive
Zonal
Cockade
Comb
0.4
0.4
0.6
0.2
0.4
0.4
1.1
0.2
0.0
0.4
0.5
0.4
0.5
0.4
0.5
0.4
0.3
0.4
0.1
0.4
0.1
0.4
0.6
0.4
0.0
0.4
Feature is present
Feature is absent
Boiling
Non boiling
Figure 10

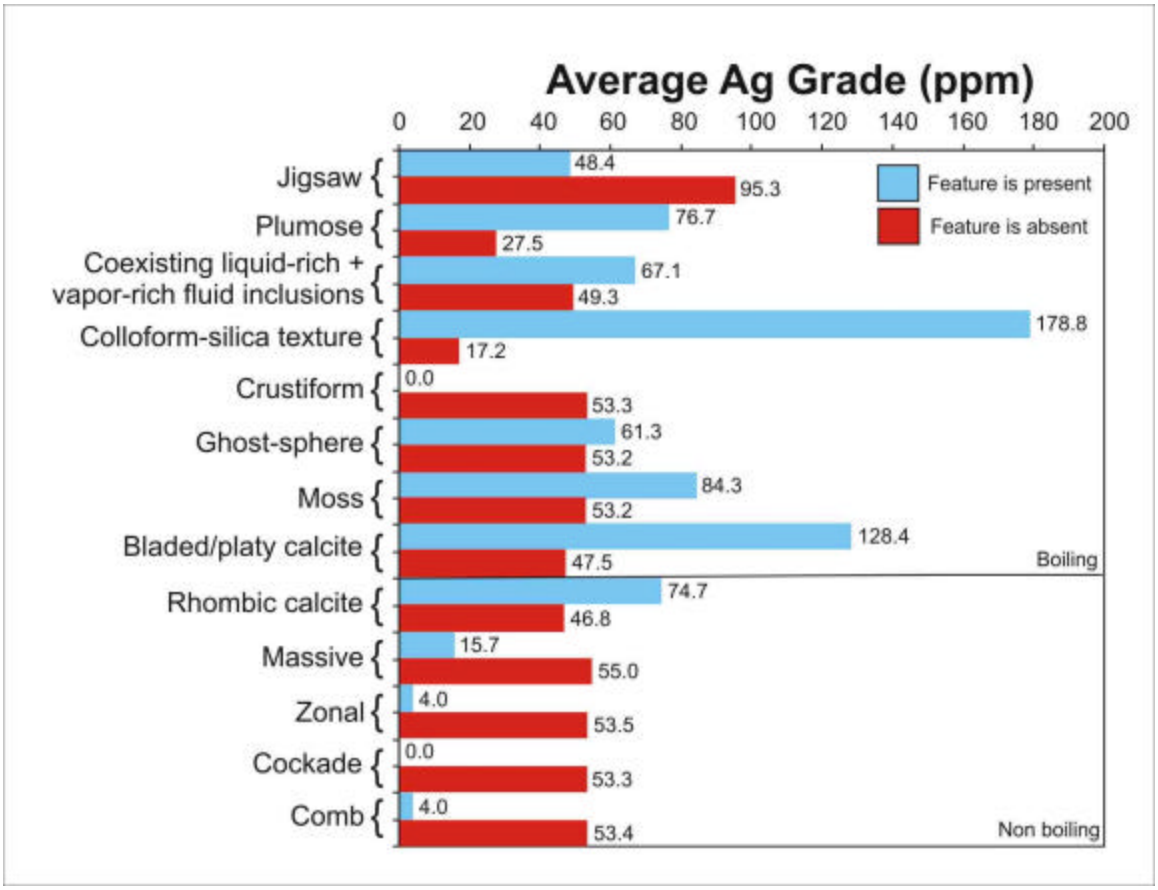
Average Ag Grade (ppm)
0
20
40
60
80
100
120
140
160
180
200
Jigsaw
48.4
95.3
Plumose
76.7
27.5
Coexisting liquid-rich + vapor-rich fluid inclusions
67.1
49.3
Colloform-silica texture
178.8
17.2
Crustiform
0.0
53.3
Ghost-sphere
61.3
53.2
Moss
84.3
53.2
Bladed/platy calcite
128.4
47.5
Rhombic calcite
74.7
46.8
Massive
15.7
55.0
Zonal
4.0
53.5
Cockade
0.0
53.3
Comb
4.0
53.4
Feature is present
Feature is absent
Boiling
Non boiling
Figure 11

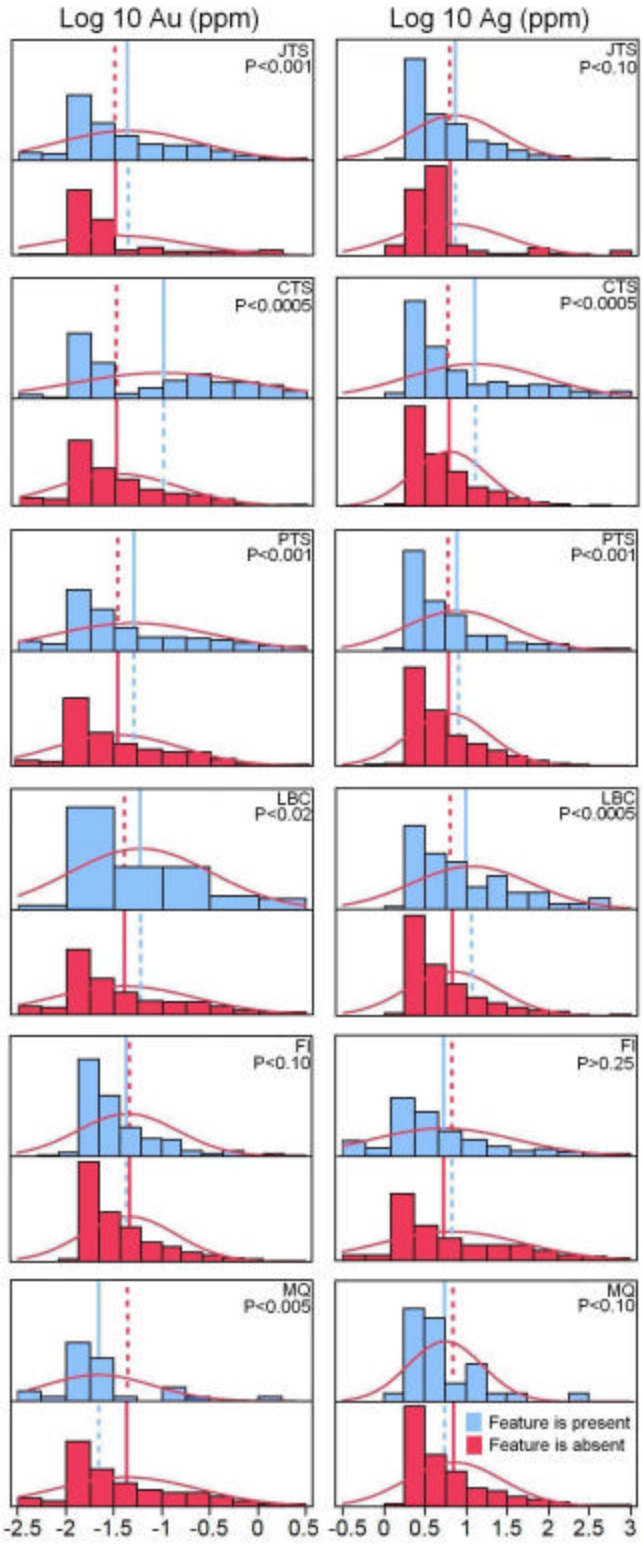
Log 10 Au (ppm)
Log 10 Ag (ppm)
JTS
P<0.001
JTS
P<0.10
CTS
P<0.0005
CTS
P<0.0005
PTS
P<0.001
PTS
P<0.001
LBC
P<0.02
LBC
P<0.0005
FI
P<0.10
FI
P>0.25
MQ
P<0.005
MQ
P<0.10
Feature is present
Feature is absent
-2.5 -2 -1.5 -1 -0.5 0 0.5
-0.5 0 0.5 1 1.5 2 2.5 3

Figure 12

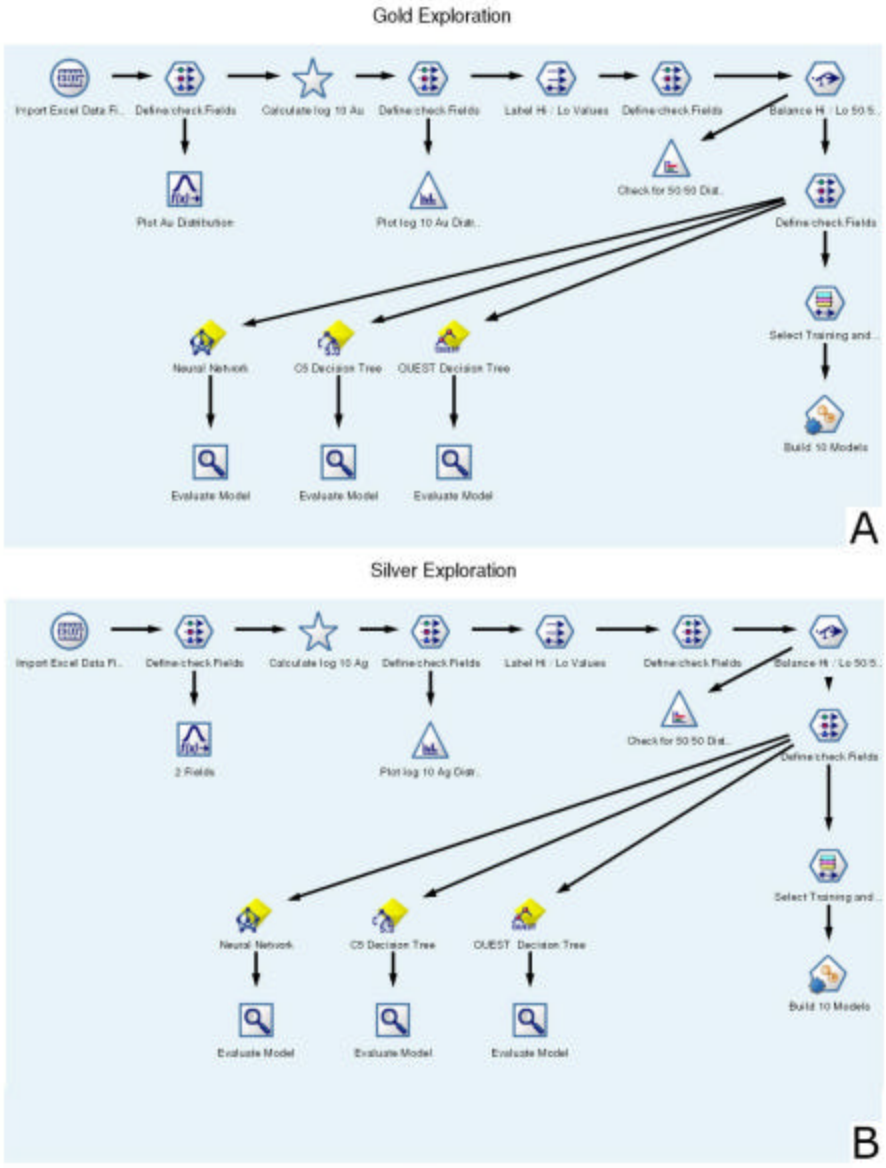
Gold Exploration
Import Excel Data Fi...
Define/check Fields
Calculate log 10 Au
Define/check Fields
Label Hi / Lo Values
Define/check Fields
Balance Hi / Lo 50:5...
Plot Au Distribution
Plot log 10 Au Distr...
Check for 50:50 Dist...
Define/check Fields
Select Training and...
Neural Network
C5 Decision Tree
QUEST Decision Tree
Build 10 Models
Evaluate Model
Evaluate Model
Evaluate Model
A
Silver Exploration
Import Excel Data Fi...
Define/check Fields
Calculate log 10 Ag
Define/check Fields
Label Hi / Lo Values
Define/check Fields
Balance Hi / Lo 50:5...
2 Fields
Plot log 10 Ag Distr...
Check for 50:50 Dist...
Define/check Fields
Select Training and...
Neural Network
C5 Decision Tree
QUEST Decision Tree
Build 10 Models
Evaluate Model
Evaluate Model
Evaluate Model
B

Figure 13

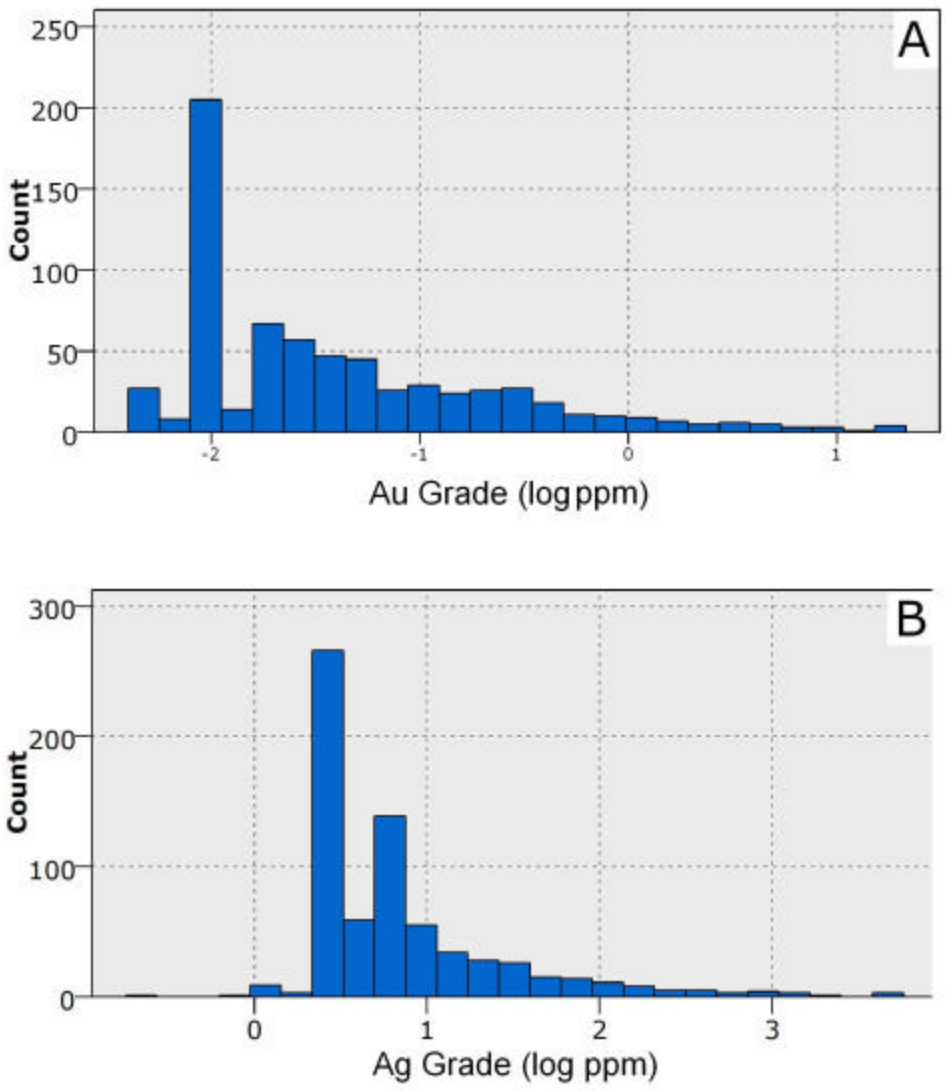
A
250
200
150
100
50
0
Count
-2
-1
0
1
Au Grade (log ppm)
B
300
200
100
0
Count
0
1
2
3
Ag Grade (log ppm)

Figure 14

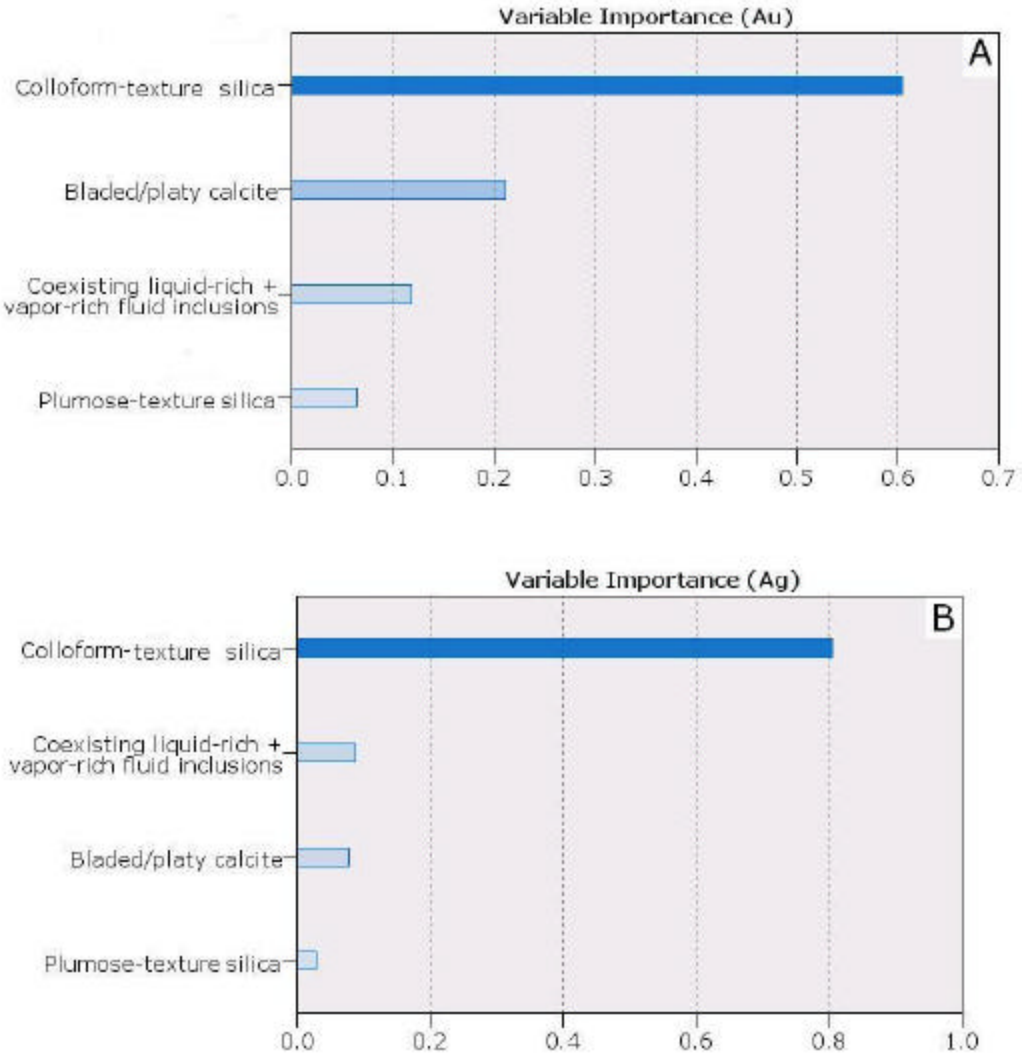
Variable Importance (Au)
A
Colloform-texture silica
Bladed/platy calcite
Coexisting liquid-rich + vapor-rich fluid inclusions
Plumose-texture silica
0.0
0.1
0.2
0.3
0.4
0.5
0.6
0.7
Variable Importance (Ag)
B
Colloform-texture silica
Coexisting liquid-rich + vapor-rich fluid inclusions
Bladed/platy calcite
Plumose-texture silica
0.0
0.2
0.4
0.6
0.8
1.0

Figure 15

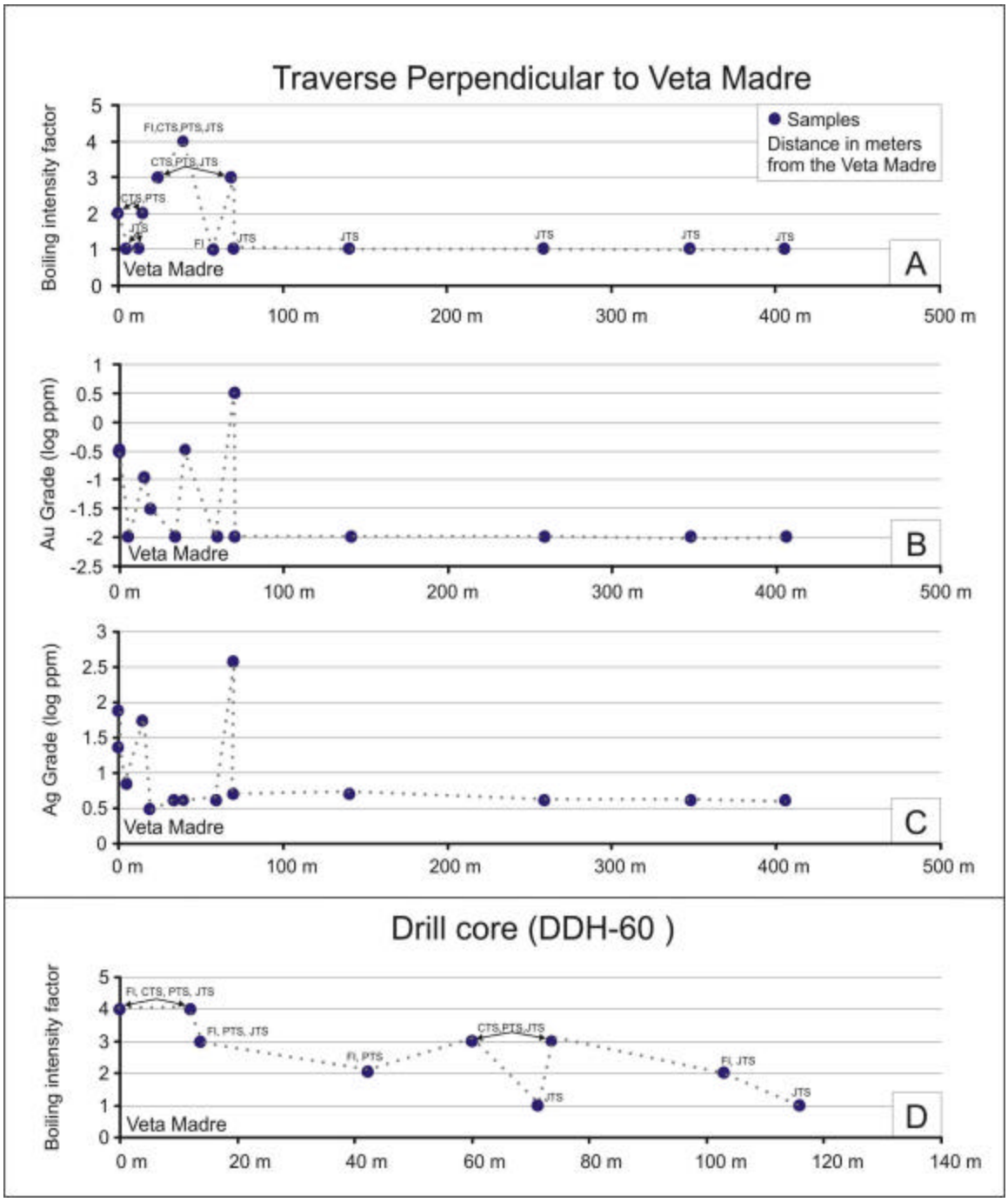
Traverse Perpendicular to Veta Madre
Boiling intensity factor
Samples
Distance in meters from the Veta Madre
FI,CTS,PTS,JTS
CTS,PTS,JTS
CTS,PTS
JTS
FI
Veta Madre
A
0 m
100 m
200 m
300 m
400 m
500 m
Au Grade (log ppm)
B
Ag Grade (log ppm)
C
Drill core (DDH-60)
FI, CTS, PTS, JTS
FI, PTS, JTS
FI, PTS
FI, JTS
D
0 m
20 m
40 m
60 m
80 m
100 m
120 m
140 m

Figure 16

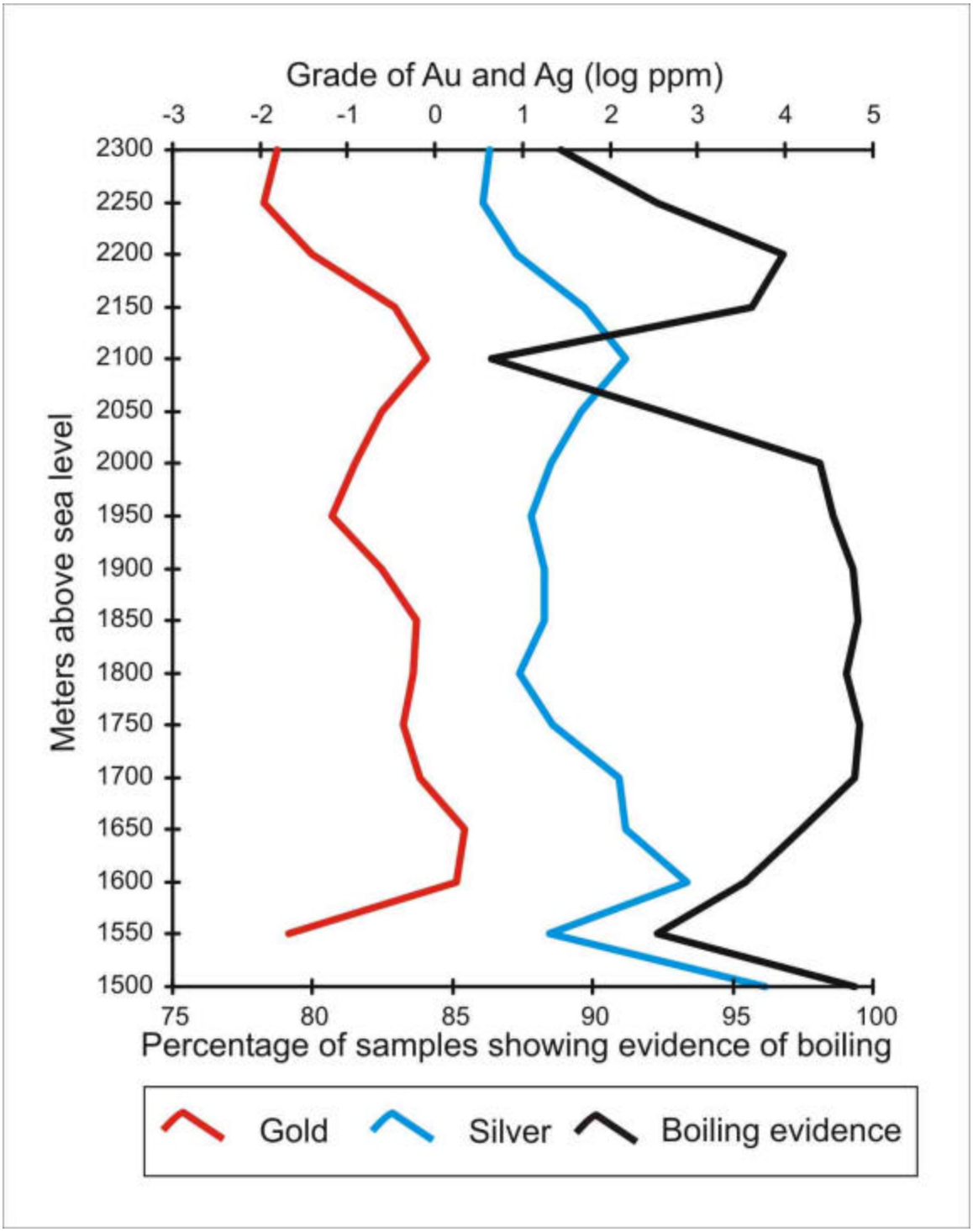
Grade of Au and Ag (log ppm)
-3
-2
-1
0
1
2
3
4
5
2300
2250
2200
2150
2100
2050
2000
1950
1900
1850
1800
1750
1700
1650
1600
1550
1500
Meters above sea level
75
80
85
90
95
100
Percentage of samples showing evidence of boiling
Gold
Silver
Boiling evidence

Figure 17